

# 8

## Quantum chromodynamics

The quark model of hadrons, developed by Gell-Mann and Zweig, began to be taken seriously in the mid to late 1960s. The discovery of scaling in deep inelastic electron–nucleon reactions in the late 1960s seemed to imply that at very short distances, or very high momentum transfers, the nucleon constituents (valence quarks) behaved like weakly interacting point particles. However, the interactions between quarks had to be very strong at long distances, or small momentum transfers, to confine them in hadrons and thus explain the non-observation of isolated quarks. Politzer [1] and Gross and Wilczek [2], who received the Nobel prize in 2004, showed that the only renormalizable field theory of quarks that had the property of an increasing force at long distance and a decreasing force at short distance was of the type discovered by Yang and Mills [3]. Quarks must be spin-1/2 fermions, with fractional electric charge, and must come in three colors (a new quantum charge akin to electric charge) in order to explain the systematics of hadron spectroscopy. Interactions between quarks are mediated by gluons (the glue which holds them together). Gluons are massless spin-1 bosons, as are photons, but unlike photons they interact among themselves directly (via point interactions) because they also carry a color charge. Such theories are called nonabelian gauge theories. This theory of quarks and gluons, quantum chromodynamics (QCD), is the accepted theory of the strong interactions. Unfortunately, it has been very difficult to make quantitative predictions with QCD, owing to its complexity and peculiar properties. For a more thorough discussion of the history of QCD and its experimental support see Close [4].

During the mid to late 1970s it was realized that there should be a qualitative change in the properties of hadronic matter as the temperature or density is increased. A dilute system could be described in terms of pions, nucleons, and other hadrons. In a very dense system such extended

composite particles would overlap, and quarks and gluons would be free to roam. There might even be a color-deconfinement phase transition at a temperature of several hundred MeV or a baryon density of around ten times the normal nuclear density. A phase transition from hadron gas to quark–gluon plasma requires a very large energy density. Such a transition could have occurred in the very early universe during the first microsecond of the big bang, or it could occur in the interior of a neutron star or during the collisions of large nuclei at very high energy in terrestrial accelerators.

The outline of this chapter is as follows. In Section 8.1 the Lagrangian of QCD is discussed as well as the functional integral representation of the partition function, including ghosts. Section 8.2 contains a brief discussion of asymptotic freedom, whereby the effective coupling decreases to zero logarithmically at short distance. In Sections 8.3 and 8.4 the perturbative evaluation of the thermodynamic potential at high temperature and density is surveyed and all known results are summarized. Section 8.5 discusses various limits of the gluon propagator, in various gauges that are useful in linear response analyses. Instantons are nonperturbative, topological, excitations which contribute to the thermodynamic potential, and a short introduction to them is given in Section 8.6. Unresolved infrared problems which appear at high order in perturbation theory are discussed in Section 8.7. Strange cold quark matter is analyzed in Section 8.8. Finally, the very interesting problem of color superconductivity is studied in Section 8.9. Applications of QCD to neutron stars, the big bang, and high-energy heavy ion collisions will be made in later chapters.

## 8.1 Quarks and gluons

Quarks must come in three colors (color being a new, strong-interaction, quantum number) in order that we may construct the observed hadrons without violating the Pauli exclusion principle. The color gauge group of QCD is  $SU(3)$ . However, we may base our analysis more generally on the group  $SU(N)$ ,  $N = 2, 3, \dots$ . The generators of the group are written as  $G^a$ , where the index  $a$  runs in integral steps from 1 to  $N^2 - 1$ . The generators satisfy the commutation relations

$$[G^a, G^b] = if^{abc}G^c \quad (8.1)$$

where the  $f^{abc}$  are the group structure constants. For example, for  $SU(2)$  the group generators may be represented by the  $2 \times 2$  Pauli matrices and for  $SU(3)$  by the  $3 \times 3$  Gell-Mann matrices.

The gauge field  $A_a^\mu$  carries color with a color index  $a = 1, \dots, N^2 - 1$ . The field strength is

$$F_a^{\mu\nu} = \partial^\mu A_a^\nu - \partial^\nu A_a^\mu - gf_{abc}A_b^\mu A_c^\nu \quad (8.2)$$

Here, the dimensionless coupling  $g$  enters. Under an infinitesimal gauge transformation  $\alpha_a(\mathbf{x}, t)$ , the gluon field transforms as

$$A_a^\mu \rightarrow A_a^\mu + g f_{abc} A_b^\mu \alpha_c - \partial^\mu \alpha_a \quad (8.3)$$

The field strength is not invariant, unlike in QED, since

$$F_a^{\mu\nu} \rightarrow F_a^{\mu\nu} + g f_{abc} F_b^{\mu\nu} \alpha_c \quad (8.4)$$

However, its square is invariant since  $F_a^{\mu\nu} F_{\mu\nu}^a \rightarrow F_a^{\mu\nu} F_{\mu\nu}^a$ .

The quarks come in  $N$  different colors, so the quark field  $\psi$  has a color index  $i$  which runs from 1 to  $N$  (where  $N = 3$  for SU(3)). The QCD Lagrangian is

$$\mathcal{L} = \bar{\psi}(i\partial - M - g\mathcal{A}_a G^a)\psi - \frac{1}{4}F_a^{\mu\nu} F_{\mu\nu}^a \quad (8.5)$$

The first term is the kinetic energy of the quarks. The second term is the quark mass matrix, which is diagonal in flavor space (that is, referring to the  $u, d, s, c, \dots$  quarks). The third term is the minimal coupling of the quarks to the gluons. (Notice the suppression of the quark color indices in (8.5). If  $G^a$  is represented by an  $N \times N$  matrix then  $\psi$  is represented by an  $N$ -dimensional column vector in color space.) In order for this coupling to be gauge invariant the quark field must transform as

$$\psi \rightarrow \exp(igG^a\alpha_a)\psi \quad (8.6)$$

The last term in (8.5) is gauge invariant by the construction of  $F_a^{\mu\nu}$ . When  $g = 0$ , (8.5) describes massive noninteracting quarks and  $N^2 - 1$  massless noninteracting “photons”.

The strong interactions conserve baryon number and electric charge. They also conserve quark flavor (such as strangeness), but the weak interactions allow for flavor change. Color charge is conserved by all known interactions. The color current density is

$$j_{(c)\mu}^a = g \left( \bar{\psi} \gamma_\mu G^a \psi + f^{abc} F_{\mu\nu}^b A_c^\nu \right) = \partial^\nu F_{\nu\mu}^a \quad (8.7)$$

The second equality follows from the Lagrange equations of motion for  $A_a^\mu$ . The conservation law  $\partial^\mu j_{(c)\mu}^a = 0$  follows from the antisymmetry of the field strength in its two Lorentz indices. The color charge generators are

$$Q_{(c)}^a = \int d^3x j_{(c)0}^a \quad (8.8)$$

The non-observation of isolated quarks or gluons leads us to postulate that only aggregates of quarks and gluons with zero net color charge, or color singlets, have finite energy. Aggregates with net color should have infinite energy. This would explain their absence. This color confinement

is a generally accepted consequence of QCD but apparently has never been rigorously established.

Quantization proceeds in a way parallel to that of QED, discussed in Section 5.1. Equation (5.24) corresponds to the QCD formula

$$Z = \int [dA_a^\mu][d\bar{\psi}][d\psi]\delta(F^b) \det\left(\frac{\partial F^c}{\partial \alpha^d}\right) \exp\left(\int_0^\beta d\tau \int d^3x (\mathcal{L} + \bar{\psi}\mu\gamma^0\psi)\right) \tag{8.9}$$

The number of polarization degrees of freedom of the gluons is  $2N_g = 2(N^2 - 1)$  and  $F^b$  is the gauge fixing function; there is one for each  $b = 1, \dots, N^2 - 1$ . Summation over quark color and flavor indices is implied.

One set of gauges that is often used is the set of covariant gauges

$$F^a = \partial^\mu A_\mu^a - f^a(\mathbf{x}, \tau) = 0 \tag{8.10}$$

Under the infinitesimal gauge transformation (8.3),

$$F^a \rightarrow \partial^\mu \left( A_\mu^a + g f^{abc} A_\mu^b \alpha^c - \partial_\mu \alpha^a \right) - f^a \tag{8.11}$$

Then the argument of the determinant is

$$\frac{\partial F^c}{\partial \alpha^d} = -\partial^2 \delta^{cd} + g f^{cbd} \partial^\mu A_\mu^b \tag{8.12}$$

As usual, we multiply  $Z$  by

$$\exp\left(-\frac{1}{2\rho} \int d\tau \int d^3x f_a^2\right)$$

and integrate over  $f^a$  to obtain

$$Z = \int [dA_a^\mu][d\bar{\psi}][d\psi] \det\left(-\partial^2 \delta^{ac} + g f^{abc} \partial^\mu A_\mu^b\right) \times \exp\left[\int d\tau \int d^3x \left(\mathcal{L} + \bar{\psi}\mu\gamma^0\psi - \frac{1}{2\rho}(\partial^\mu A_\mu^a)^2\right)\right] \tag{8.13}$$

As in (5.26) and (5.34), we introduce ghost fields  $\bar{C}_a$  and  $C_a$  to represent the determinant in functional integral form:

$$Z = \int [dA_a^\mu][d\bar{\psi}][d\psi][d\bar{C}_a][dC_a] \exp\left(\int d\tau \int d^3x \mathcal{L}_{\text{eff}}\right) \tag{8.14}$$

where

$$\mathcal{L}_{\text{eff}} = \mathcal{L} - \frac{1}{2\rho}(\partial^\mu A_\mu^a)^2 + g f^{abc} \bar{C}_a \partial_\mu A_\mu^b C_c + \bar{\psi}\mu\gamma^0\psi + \partial_\mu \bar{C}_a \partial^\mu C_a$$

In the covariant gauges the ghost field does not decouple from the gluon field. The ghost field integration cannot be factored out.

In Table 8.1 the diagrammatic rules for QCD in the covariant gauges are listed. Table 8.2 contains a listing of the properties of the six quarks. The numerical values of the quark masses depend on the precise way in which they are defined, since freely propagating quarks do not exist. The three light quark masses are evaluated at an  $\overline{\text{MS}}$  scale of 2 GeV, while the three heavy quark masses are evaluated at their own mass.

## 8.2 Asymptotic freedom

The renormalization-group running coupling for massless  $\lambda\phi^4$  theory,  $\lambda_R$ , was discussed in Section 4.2. From (4.25) we saw that the effective coupling grows at high energy, or equivalently at short distance. The physical interpretation is that a point charge is shielded, or screened, by virtual pair production in the vacuum. As we approach the source of the charge, we penetrate the screening cloud surrounding it. The effective charge we see becomes larger due to the loss of screening. In a sense this is like penetrating the electron cloud surrounding an atomic nucleus. The difference is that the atomic electrons are real particles nearly on their mass shell. Electronic screening is essentially a classical effect. The increase in the renormalization-group charge is effected in the lowest approximation by virtual particles and so is a purely quantum effect.

To lowest order in the coupling constant, a  $\beta$ -function is either positive (the charge grows at short distance) or negative (the charge decreases at short distance). Until 1973, examples of only the former were known. The discovery that only nonabelian gauge theories allow for a negative  $\beta$ -function is credited to Politzer [1] and to Gross and Wilczek [2]. They showed that QCD yields a charge that decreases at short distance, an effect called asymptotic freedom that is required by experiment. This discovery was not anticipated by any simple intuitive reasoning. Let us examine the renormalization-group as it applies to QCD with massless quarks and in the set of covariant gauges.

The renormalization-group equation for the irreducible vertex function for  $n$  gluon and  $n'$  massless quark fields is (see the discussion leading to (4.13))

$$\left( M \frac{\partial}{\partial M} + \beta(g, \rho) \frac{\partial}{\partial g} + \delta(g, \rho) \frac{\partial}{\partial \rho} + n\gamma_A(g, \rho) + n'\gamma_\psi(g, \rho) \right) \times \Gamma^{n, n'}(p_1, \dots, p_{n+n'}; g, \rho, M) = 0 \quad (8.15)$$

Here  $\delta$  is the “ $\beta$ -function” corresponding to the gauge parameter  $\rho$ .

Table 8.1. Bare propagators and vertices in QCD in covariant gauges

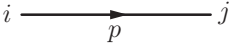
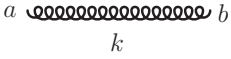

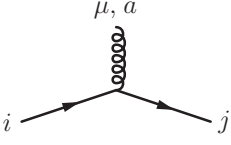
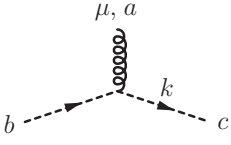
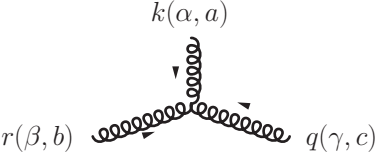
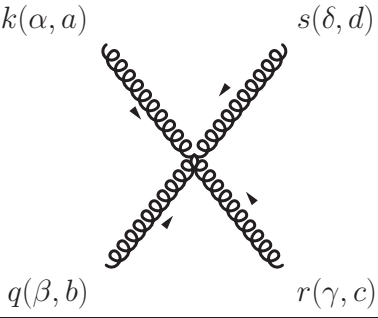
Quark		$\mathcal{G}_{ij} = \frac{\delta_{ij}}{\not{p} - m}, p_0 = i\omega_n + \mu$
Gluon		$\mathcal{D}^{\mu\nu} = \frac{\delta_{ab}}{k^2} \left( g^{\mu\nu} - \frac{(1 - \rho)k^\mu k^\nu}{k^2} \right)$
Ghost		$\mathcal{W}_{ab} = \frac{\delta_{ab}}{k^2}$
		$\Gamma_0^F = g\gamma^\mu G_{ij}^a$
		$\Gamma_0^G = -igf_{abc}k_\mu$
		$\Gamma_{0(3)}^V = igf_{abc} [g_{\beta\gamma}(r - q)_\alpha + g_{\alpha\beta}(k - r)_\gamma + g_{\gamma\alpha}(q - k)_\beta]$
		$\Gamma_{0(4)}^V = -g^2 [f_{ade}f_{ebc}(g_{\alpha\beta}g_{\delta\gamma} - g_{\alpha\gamma}g_{\delta\beta}) + f_{abe}f_{edc}(g_{\alpha\delta}g_{\beta\gamma} - g_{\alpha\gamma}g_{\delta\beta}) + f_{ace}f_{edb}(g_{\alpha\delta}g_{\beta\gamma} - g_{\alpha\beta}g_{\delta\gamma})]$

Table 8.2. Quark properties

Flavor	Electric charge	Baryon number	Mass
$u$ (up)	$2/3$	$1/3$	3 MeV
$d$ (down)	$-1/3$	$1/3$	7 MeV
$s$ (strange)	$-1/3$	$1/3$	120 MeV
$c$ (charm)	$2/3$	$1/3$	1.2 GeV
$b$ (bottom)	$-1/3$	$1/3$	4.25 GeV
$t$ (top)	$2/3$	$1/3$	175 GeV

There is a Ward identity for QCD which states that the longitudinal part of the inverse gluon propagator is not altered by interactions. That is,

$$\Gamma_L^{2,0} = \frac{p^\mu p^\nu}{\rho} \quad (8.16)$$

This is the same as in QED (see (5.46)). Application of (8.15) to (8.16) then yields the relation

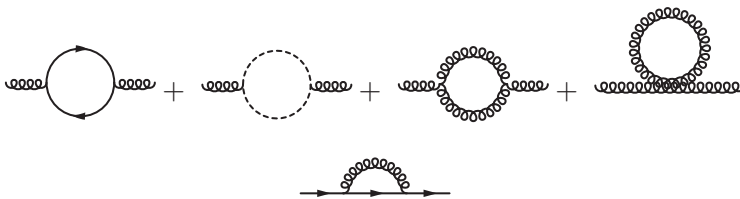
$$\delta(g, \rho) = 2\rho\gamma_A(g, \rho) \quad (8.17)$$

This points to the advantage of the Landau gauge  $\rho = 0$ ; in this gauge  $\delta(g, 0) = 0$ . Hence, starting with  $\rho = 0$  we are guaranteed that after renormalization  $\rho = 0$  will remain true, on account of the renormalization group equation

$$M \frac{\partial \bar{\rho}}{\partial M} = \delta(\bar{g}, \bar{\rho}) \quad (8.18)$$

Otherwise, we must keep  $\rho$  arbitrary in our equations. For example,  $\rho = 1$  will not remain as such under application of the renormalization group.

The  $\gamma$ 's may be obtained most directly from  $\Gamma_T^{2,0}$  and  $\Gamma^{0,2}$ . To lowest order in  $g$  we must evaluate the following diagrams:



If these are normalized to have their free-field values at  $p^2 = -M^2$  (according to Euclidean momentum subtraction) then

$$\Gamma_T^{2,0} = (p^2 g^{\mu\nu} - p^\mu p^\nu) \left\{ 1 + \left[ \left( \frac{13}{6} - \frac{1}{2}\rho \right) c_1 - \frac{4}{3}c_2 \right] \frac{g^2}{16\pi^2} \ln \left( -\frac{p^2}{M^2} \right) \right\} \tag{8.19}$$

$$\Gamma^{0,2} = \not{p} \left[ 1 - \rho c_1 \frac{g^2}{16\pi^2} \ln \left( -\frac{p^2}{M^2} \right) \right] \tag{8.20}$$

The  $c$ 's are given by

$$\begin{aligned} f_{acd}f_{bcd} &= c_1 \delta_{ab} = N \delta_{ab} \\ N_f \text{Tr } G_a G_b &= c_2 \delta_{ab} = \frac{1}{2} N_f \delta_{ab} \end{aligned} \tag{8.21}$$

and  $N_f$  is the number of quark flavors. If we apply (8.15) to (8.19) and (8.20), and after differentiation set  $p^2 = -M^2$ , we can solve for the  $\gamma$ 's:

$$\gamma_A = \frac{g^2}{16\pi^2} \left[ \left( \frac{13}{6} - \frac{1}{2}\rho \right) c_1 - \frac{4}{3}c_2 \right] \tag{8.22}$$

$$\gamma_\psi = -\frac{g^2}{16\pi^2} \rho c_1 \tag{8.23}$$

It is not possible to determine the  $\beta$ -function in these covariant gauges with knowledge of the two-point functions (propagators) alone.

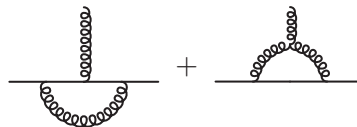
Knowledge of a three-point function would suffice to determine  $\beta$ . From the following diagrams,



we compute

$$\begin{aligned} \Gamma^{3,0} &= -igf_{abc}(g_{\beta\gamma}p_\alpha + g_{\alpha\beta}p_\gamma - 2g_{\gamma\alpha}p_\beta) \\ &\times \left\{ 1 + \left[ \left( \frac{17}{12} - \frac{3}{4}\rho \right) c_1 - \frac{4}{3}c_2 \right] \frac{g^2}{16\pi^2} \ln \left( -\frac{p^2}{M^2} \right) \right\} \end{aligned} \tag{8.24}$$

and from





we compute

$$\Gamma^{1,2} = -g\gamma^\mu G_a \left[ 1 - \left( \frac{3}{4} + \frac{5}{4}\rho \right) c_1 \frac{g^2}{16\pi^2} \ln \left( -\frac{p^2}{M^2} \right) \right] \quad (8.25)$$

These are computed with external momenta  $(p_1, p_2, p_3) = (0, -p, p)$  and normalized at  $p^2 = -M^2$ . Application of (8.15) to either (8.24) or (8.25) yields the lowest-order renormalization-group  $\beta$ -function,

$$\beta = -\frac{g^2}{48\pi^2} (11N - 2N_f) \quad (8.26)$$

This will be negative, and the running coupling  $g$  will decrease with increasing energy, as long as  $N_f < 5.5N$ . This condition is fulfilled for SU(3), with six quark flavors.

It is worthwhile remarking that knowledge of the gluon two-point function in the Coulomb gauge ( $\nabla \cdot \mathbf{A}_a = 0$ ) and the axial gauge ( $n \cdot A = 0$ , where  $n$  is a fixed four-vector) is sufficient to determine  $\beta$ . The reason is that the noncovariance of these gauges provides a tensorial structure for the gluon propagator and self-energy that requires two independent scalar functions, even in the vacuum (see Sections 5.4 and 6.3). These two independent scalar functions then allow the determination of both  $\gamma_A$  and  $\beta$ . The result is identical to (8.26).

The renormalization-group running coupling is determined by (see Section 4.2)

$$M \frac{\partial \bar{g}}{\partial M} = \beta(\bar{g}) \quad (8.27)$$

with solution

$$\bar{\alpha} = \frac{\bar{g}^2}{4\pi} = \frac{12\pi}{(11N - 2N_f) \ln(M^2/\Lambda^2)} \quad (8.28)$$

This explicitly displays asymptotic freedom:  $\bar{\alpha} \rightarrow 0$  as  $M \rightarrow \infty$ . Notice the absence of any intrinsic coupling “constant” on the right-hand side of (8.28). In its place as the free parameter of the theory is the QCD energy scale  $\Lambda$ . The numerical value of  $\Lambda$  is, however, dependent on the gauge and on the renormalization scheme chosen (for example, this might be the choice used in (8.24) and (8.25)). This is seen in higher order.

Finite quark masses can be incorporated into the renormalization-group analysis by adding to the differential operator in (8.15) a term

$$\gamma_m \left( g, \rho, \frac{m_f}{M} \right) m_f \frac{\partial}{\partial m_f}$$

for each quark flavor  $f$ . That is,  $m_f/M$  is treated as a dimensionless coupling constant. The quark mass may be defined by

$$\mathcal{G}^{-1}|_{p^2=-M^2} = \not{p} - m \quad (8.29)$$

This is one possible renormalization prescription, but there exist others. A direct computation of  $\beta$  and  $\gamma_m$  in the Landau gauge yields [5]

$$M \frac{\partial g}{\partial M} = \beta = -\frac{g^3}{48\pi^2} \left[ 11N - \frac{2}{3} \sum_f B_0 \left( \frac{m_f^2}{M^2} \right) \right] \quad (8.30)$$

where

$$B_0(x) = 1 - 6x + 12 \left( \frac{x^2}{y} \right) \ln \left( \frac{y+1}{y-1} \right) \\ y = \sqrt{1+4x} \quad (8.31)$$

and

$$\frac{M}{m} \frac{\partial m}{\partial M} = \gamma_m = -\frac{g^2}{2\pi^2} C_0 \left( \frac{m^2}{M^2} \right) \quad (8.32)$$

$$C_0(x) = 1 - x \ln(1+x^{-1}) \quad (8.33)$$

Good approximations for  $B_0$  and  $C_0$  are

$$B_0(x) \simeq (1+5x)^{-1} \\ C_0(x) \simeq (1+2x)^{-1} \quad (8.34)$$

(We have now removed the overbar from  $g$  and  $m$  and will denote the running coupling and mass by  $g$  and  $m$  for notational simplicity.)

In general, (8.30) and (8.32) form a set of  $N_f + 1$  coupled first-order nonlinear differential equations that must be solved numerically. The basic features of these equations are readily understood in the following way. The running coupling can be written as

$$\frac{g^2}{4\pi} = \frac{12\pi}{[11N - 2N_f^{\text{eff}}(M)] \ln(M^2/\Lambda^2)} \quad (8.35)$$

where

$$N_f^{\text{eff}}(M) \simeq \frac{1}{\ln(M^2/\Lambda^2)} \sum_f \frac{M^2 + m_f^2(M)}{\Lambda^2 + m_f^2(M)} \quad (8.36)$$

is the effective number of quark flavors at the energy scale  $M$ . Equations (8.35) and (8.36) form a solution to (8.30) valid to the lowest order in  $g$ . If  $m_f(M)$  is small then it contributes to  $\beta$ , but if it is large then it decouples. That is, if the quark mass is large compared with the energy

scale of interest then there is insufficient energy for pair production, so that flavor does not add to the charge screening.

As an example, consider the first three quark flavors with  $m_u = m_d = 0$  but  $m_s \neq 0$ . We look at high energy where  $M \gg m_s$ . Then  $g^2/4\pi \simeq 2\pi/[9\ln(M/\Lambda)]$  can be inserted into (8.32):

$$\frac{dm_s}{dM} = -\frac{4}{9\ln(M/\Lambda)} \frac{m_s}{M} \quad (8.37)$$

This has the solution

$$m_s(M) = m_{s0} \left[ \frac{\ln(M_0/\Lambda)}{\ln(M/\Lambda)} \right]^{4/9} \quad (8.38)$$

where  $m_{s0}$  is the mass at the scale  $M_0$ . The monotonic decrease in quark mass with increasing energy is in fact a general feature of (8.32), since  $\gamma_m < 0$ .

The  $\beta$ -function has been computed to two loops, that is, to order  $g^5$  (the reader is referred to [6] for a more detailed discussion of massive quarks). For massless quarks [7],

$$\begin{aligned} \beta &= -(11N - 2N_f) \frac{g^3}{48\pi^2} - \left( 34N^2 - 13NN_f + 3\frac{N_f}{N} \right) \frac{g^5}{768\pi^4} \\ &\equiv -\beta_0 g^3 - \beta_1 g^5 \end{aligned} \quad (8.39)$$

which is still gauge and prescription independent. An approximate solution of the renormalization-group equation is

$$\alpha_2(M) = \alpha_1(M) - 4\pi \left( \frac{\beta_1}{\beta_0} \right) \alpha_1^2(M) \ln \left( \frac{1}{\alpha_1(M)} \right) \quad (8.40)$$

where  $\alpha_1(M) = 1/[4\pi\beta_0 \ln(M^2/\Lambda^2)]$  is the lowest-order solution. Corrections to (8.40) are of order  $\alpha_1^3(M) \sim [1/\ln(M^2/\Lambda^2)]^3$ . For QCD with  $N_f = 3$ ,  $\alpha_2(M) = \alpha_1(M) + 0.0354 \alpha_1^2(M) \ln \alpha_1(M)$ . Thus, when  $\alpha_1(M) \ll 1$  we have  $\alpha_2(M) \simeq \alpha_1(M)$  to rather good accuracy.

The thermodynamic potential  $\Omega$  must be independent of gauge and of renormalization prescription since it is a measurable quantity. However, the way this works in practice can be rather subtle. For example, if we work in a covariant gauge then

$$\frac{d}{d\rho} \Omega(g(\rho), \rho) = \left( \frac{\partial}{\partial \rho} + \frac{\partial g}{\partial \rho} \frac{\partial}{\partial g} \right) \Omega(g(\rho), \rho) = 0 \quad (8.41)$$

must hold, not  $\partial\Omega(g, \rho)/\partial\rho = 0$ . The reason is that  $g$  depends on the gauge and on the renormalization prescription used to render it finite from its bare value.

### 8.3 Perturbative evaluation of partition function

Since the effective QCD coupling goes to zero logarithmically at short distances, it is reasonable to attempt a perturbative expansion of the thermodynamic potential at high energy density [8, 9, 10]. In this and the next section we summarize the results so far obtained. Possible limits to the usefulness of perturbation theory will be discussed in later sections, as will some applications of the formulae obtained here. In the following discussion we quote perturbative results for the pressure  $P(T, \mu)$ . The entropy density  $s = \partial P / \partial T$ , flavor densities  $n_f = \partial P / \partial \mu_f$ , and energy density  $\epsilon = -P + Ts + \sum_f \mu_f n_f$  are computed straightforwardly.

To zero order in the coupling, the QCD plasma is an ideal gas of gluons and quarks. The pressure can be written down immediately from (1.31) and (1.32):

$$P_0 = \frac{\pi^2}{45} N_g T^4 + \frac{N}{3\pi^2} \sum_f \int_0^\infty \frac{dp p^4}{E_p} N_F(p) \tag{8.42}$$

where  $N_g = N^2 - 1$  is the number of gluons, which is eight for SU(3). When  $m_f = 0$  the integral in (8.42) can be evaluated in closed form. The contribution to the pressure is

$$P_{0f}(m_f = 0) = N \left( \frac{7\pi^2 T^4}{180} + \frac{\mu_f^2 T^2}{6} + \frac{\mu_f^4}{12\pi^2} \right) \tag{8.43}$$

The exchange corrections to the ideal gas pressure are of order  $g^2$ . The relevant diagrams are shown below:

$$-\frac{1}{2} \text{[diagram 1]} - \frac{1}{2} \text{[diagram 2]} + \frac{1}{12} \text{[diagram 3]} + \frac{1}{8} \text{[diagram 4]} \tag{8.44}$$

The diagram with the quark loop is analyzed exactly as the QED diagram in (5.39) but with the replacement  $e^2 \rightarrow g^2 \text{Tr } G_a G_a = \frac{1}{2} g^2 N_g$ . Then (5.58) to (5.61) can be taken over straightforwardly. The ghost diagram and the two pure gluon diagrams can be evaluated by means that should now be familiar. Since these are two-loop diagrams, the unrenormalized contributions will have parts that are quadratic and linear in the massless boson occupation probability  $(e^{\beta\omega} - 1)^{-1}$ . (Parts that are  $T$ -independent only renormalize the vacuum energy and these are discarded.) The subtraction procedure eliminates the linear parts. The three

diagrams contribute, in respective order,

$$\begin{aligned}
 P_2^{\text{gluon}} &= g^2 N N_g \left( \int \frac{d^3 p}{(2\pi)^3} \frac{1}{\omega} \frac{1}{e^{\beta\omega} - 1} \right)^2 \left( -\frac{1}{4} + \frac{9}{4} - 3 \right) \\
 &= -\frac{g^2}{144} N N_g T^4
 \end{aligned}
 \tag{8.45}$$

This result is gauge invariant, although the individual diagrams are not.

As in QED and in massless  $\lambda\phi^4$  theory, the next contributions are not of order  $g^4$ ; they are of order  $g^4 \ln g^2$  and  $g^3$ . These come from the set of ring diagrams

$$\frac{1}{2} \left[ \frac{1}{2} \text{ring} - \frac{1}{3} \text{ring} + \dots \right]$$

where

$$\text{ring}(\Pi) = \text{ring}(\text{gluon}) + \text{ring}(\text{ghost}) - \frac{1}{2} \text{ring}(\text{gluon, ghost}) - \frac{1}{2} \text{ring}(\text{gluon, ghost, gluon})$$

The analysis proceeds exactly in parallel with that in subsection 5.5.2. What is needed is the static infrared limit of  $\Pi^{\mu\nu}$ . This will be discussed more thoroughly in a later section, and for now we simply quote the result at  $T > 0$ ,

$$P_{\text{ring}}^{(1)} = \frac{N_g}{12\pi} T m_{\text{el}}^3$$

where

$$\begin{aligned}
 m_{\text{el}}^2 &= F(n=0, \mathbf{k} \rightarrow \mathbf{0}) = -\Pi^{00}(n=0, \mathbf{k} \rightarrow \mathbf{0}) \\
 &= g^2 \left( \frac{1}{3} N T^2 + \frac{1}{2\pi^2} \sum_f \int_0^\infty \frac{dp}{E_p} (p^2 + E_p^2) N_F(p) \right)
 \end{aligned}
 \tag{8.48}$$

is the square of the inverse screening length for color charge. When all quark masses can be neglected, we have

$$m_{\text{el}}^2 = g^2 \left[ \left( \frac{1}{3} N + \frac{1}{6} N_f \right) T^2 + \frac{1}{2\pi^2} \sum_f \mu_f^2 \right]$$

It should be noted that (8.47) and (8.48) have been obtained in the covariant gauges, in the Coulomb gauge, and in the temporal axial gauge ( $A_0^a = 0$ ). If, in addition, the lowest-order momentum dependence of  $\Pi^{00}$

is retained,

$$-\Pi^{00} = m_{\text{el}}^2 - \frac{1}{4}Ng^2|\mathbf{k}|T + \dots \tag{8.50}$$

then one obtains a  $g^4 \ln g^2$  term not present in QED [11],

$$P_{\text{ring}}^{(2)} = \frac{NN_g}{65\pi^2}T^2m_{\text{el}}^2 g^2 \ln g^2 \tag{8.51}$$

However, this term is not precisely defined until the full order- $g^4$  contribution at finite temperature is determined. This will be discussed in the next section.

At  $T = 0$ , the three loop diagrams that are not already included in the ring sum are



$$\tag{8.52}$$

The first two diagrams are analogous to those of QED, (5.77), but the last is peculiar to QCD on account of the three-gluon coupling. These diagrams are technically quite involved, owing to overlapping ultraviolet divergences. The interested reader is referred to Freedman and McLerran [12] and Baluni [13] for their evaluations. The result of summing the ring diagrams (8.46) together with (8.52) is

$$\begin{aligned}
 P_{\text{ring}} + P_4 = & \frac{1}{4\pi^2} \left\{ \sum_f \mu_f^4 \left[ N_g \frac{11N - 2N_f}{3} \left( \frac{\alpha(M)}{4\pi} \right)^2 \ln \left( \frac{\mu_f^2}{M^2} \right) \right. \right. \\
 & + N_g \left( -2.250N + 0.409N_f - 3.697 - \frac{(4.236)}{N} \right) \\
 & \left. \left. \times \left( \frac{\alpha(M)}{4\pi} \right)^2 \right] - (\boldsymbol{\mu}^2)^2 N_g \left[ 2 \ln \left( \frac{\alpha(M)}{4\pi} \right) - 0.476 \right] \right. \\
 & \left. \times \left( \frac{\alpha(M)}{4\pi} \right)^2 - N_g \bar{F}(\boldsymbol{\mu}) \left( \frac{\alpha(M)}{4\pi} \right)^2 \right\} \tag{8.53}
 \end{aligned}$$

where  $\boldsymbol{\mu} = (\mu_u, \mu_d, \mu_s, \dots)$  and

$$\begin{aligned}
 \bar{F}(\boldsymbol{\mu}) = & -2\boldsymbol{\mu}^2 \sum_f \mu_f^2 \ln \left( \frac{\mu_f^2}{\boldsymbol{\mu}^2} \right) + \frac{2}{3} \sum_{i>j} \left[ (\mu_i - \mu_j)^4 \ln \left( \frac{|\mu_i^2 - \mu_j^2|}{\mu_i \mu_j} \right) \right. \\
 & \left. + 4\mu_i \mu_j (\mu_i^2 + \mu_j^2) \ln \left( \frac{(\mu_i + \mu_j)^2}{\mu_i \mu_j} \right) - (\mu_i^4 - \mu_j^4) \ln \left( \frac{\mu_i}{\mu_j} \right) \right] \tag{8.54}
 \end{aligned}$$

These formulae were obtained in the Landau gauge using the momentum subtraction scheme; that is, the gluon self-energy was renormalized

in such a way that  $F(\bar{k}^2 = M^2, \boldsymbol{\mu} = \mathbf{0}) = G(\bar{k}^2 = M^2, \boldsymbol{\mu} = \mathbf{0}) = 0$ . The corresponding formulae for nonzero quark masses have not been computed.

It should be noticed that the pressure in (8.53) depends explicitly on the renormalization energy scale  $M$ . To avoid the large logarithms,  $\ln(\mu_f^2/M^2)$ , that would appear if  $\mu_f \rightarrow \infty$  while  $M$  is fixed, we should choose  $M$  in an optimum way. There is an arbitrariness in this, but a natural choice would be  $M^2 = \boldsymbol{\mu}^2$  and another would be  $M^2 = \boldsymbol{\mu}^2/N_f$ . Of course, if we could sum all orders of perturbation theory it would not matter. Truncating at a finite order means that we should choose an optimum  $M$  to reduce the importance of the terms neglected.

The QCD coupling  $g$  is not a fixed quantity. It depends on the gauge and on the renormalization prescription. This dependence is not apparent at order  $g^2$  but first arises at order  $g^4$ . Thus, consider two gauges and/or prescriptions labeled  $i$  and  $j$ . One can show that (see for example [14])

$$g_i^2 = g_j^2(1 + A_{ij}g_j^2 + \dots) \quad (8.55)$$

where  $A_{ij}$  is a computable number. The QCD scale  $\Lambda$  thus also depends on the gauge and/or prescription. Putting together (8.28), (8.39), and (8.55) we find that

$$\frac{\Lambda_i}{\Lambda_j} = \exp\left(\frac{A_{ij}}{2\beta_0}\right) \quad (8.56)$$

These features of QCD must be kept in mind when using high-order perturbation theory. For example, the numerical coefficient of  $\alpha^2$  in (8.53) is gauge and prescription dependent, in just such a way that when (8.55) is used the pressure is independent of gauge and prescription to this order (see also Section 8.2).

### 8.4 Higher orders at finite temperature

As we have seen previously, the simplest possible interaction yields a contribution to the pressure that is of order  $g^2$ . Owing to the summation implied by the ring diagrams, there are then contributions of order  $g^3$  and  $g^4 \ln g^2$ . By now it should be clear that one cannot determine the order of a diagram by simply counting the number of interaction vertices, if the diagram requires resummed gluons. This resummation procedure has the great advantage of curing potential infrared divergences, as already seen in Chapters 3 and 5, because in effect the resummation induces a mass which is the static infrared limit of the self-energy. Calculations of the pressure to order  $g^4$  and order  $g^5$  have used the following strategy

in order to improve the convergence of the perturbation expansion. One redefines the Lagrangian according to

$$\mathcal{L} \rightarrow \left( \mathcal{L} + \frac{1}{2} m_{\text{el}}^2 A_0^a A_0^a \delta_{p_0,0} \right) - \frac{1}{2} m_{\text{el}}^2 A_0^a A_0^a \delta_{p_0,0} \quad (8.57)$$

where  $\mathcal{L}$  is the original Lagrangian in frequency–momentum space,  $A_0$  is the zeroth component of the color gauge field, and  $p_0 = 2\pi n T i$  is the zeroth component of its momentum. With this redefinition, the term in parentheses becomes the unperturbed Lagrangian and the other term creates a thermal counterterm, necessary to avoid double-counting. Following this scheme, the  $g^4$  term receives contributions from the sub-leading part of the two-loop diagrams as well as from the leading part of the three-loop diagrams. The complete finite-temperature  $g^4$  result for gauge fields with fermions was obtained by Arnold and Zhai [14] and it is (for zero chemical potential)

$$\begin{aligned} P = & d_A T^4 \frac{\pi^2}{9} \left\{ \frac{1}{5} \left( 1 + \frac{7d_F}{4d_A} \right) \right. \\ & - \left( \frac{g}{4\pi} \right)^2 \left( C_A + \frac{5}{2} S_F \right) + \frac{16}{\sqrt{3}} \left( \frac{g}{4\pi} \right)^3 (C_A + S_F)^{3/2} \\ & + 48 \left( \frac{g}{4\pi} \right)^4 C_A (C_A + S_F) \ln \left( \frac{g}{2\pi} \sqrt{\frac{C_A + S_F}{3}} \right) \\ & - \left( \frac{g}{4\pi} \right)^4 C_A^2 \left[ \frac{22}{3} \ln \left( \frac{M}{4\pi T} \right) + \frac{38}{3} \frac{\zeta'(-3)}{\zeta(-3)} - \frac{148}{3} \frac{\zeta'(-1)}{\zeta(-1)} - 4\gamma_E + \frac{64}{5} \right] \\ & - \left( \frac{g}{4\pi} \right)^4 C_A S_F \left[ \frac{47}{3} \ln \left( \frac{M}{4\pi T} \right) + \frac{1}{3} \frac{\zeta'(-3)}{\zeta(-3)} - \frac{74}{3} \frac{\zeta'(-1)}{\zeta(-1)} \right. \\ & \quad \left. - 8\gamma_E + \frac{1759}{60} + \frac{37}{5} \ln 2 \right] \\ & - \left( \frac{g}{4\pi} \right)^4 S_F^2 \left[ -\frac{20}{3} \ln \left( \frac{M}{4\pi T} \right) + \frac{8}{3} \frac{\zeta'(-3)}{\zeta(-3)} - \frac{16}{3} \frac{\zeta'(-1)}{\zeta(-1)} \right. \\ & \quad \left. - 4\gamma_E - \frac{1}{3} + \frac{88}{5} \ln 2 \right] - \left( \frac{g}{4\pi} \right)^4 S_{2F} \left( -\frac{105}{4} + 24 \ln 2 \right) \left. \right\} \quad (8.58) \end{aligned}$$

In the equation above,  $\zeta$  is Riemann's zeta function,  $\gamma_E$  is Euler's constant, and  $M$  is the renormalization scale in the modified minimal subtraction scheme,  $\overline{\text{MS}}$ . For  $\text{SU}(N)$  with  $N_f$  fermions one may write  $d_A = N^2 - 1$ ,  $C_A = N$ ,  $d_F = NN_f$ ,  $S_F = N_f/2$ ,  $S_{2F} = (N^2 - 1)N_f/4N$ .



The extension of those techniques to one order higher by Zhai and Kastening [16] yields the  $g^5$  term:

$$\begin{aligned}
 P_5 = & \left(\frac{g}{4\pi}\right)^5 \left(\frac{C_A + S_F}{3}\right)^{1/2} \\
 & \times \left\{ C_A^2 \left[ 176 \ln\left(\frac{M}{4\pi T}\right) + 176\gamma_E - 24\pi^2 - 494 + 264 \ln 2 \right] \right. \\
 & + C_A S_F \left[ 112 \ln\left(\frac{M}{4\pi T}\right) + 112\gamma_E + 72 - 128 \ln 2 \right] \\
 & \left. + S_F^2 \left[ -64 \ln\left(\frac{M}{4\pi T}\right) - 64\gamma_E + 32 - 128 \ln 2 \right] - 144 S_{2F} \right\}
 \end{aligned}
 \tag{8.59}$$

As will be discussed in Section 8.7, the hopes of pursuing an order-by-order expansion in finite-temperature QCD are too optimistic. The analytic expansion has serious infrared problems. Postponing a discussion of these aspects, it suffices here to say that for the pressure, this problem is met at order  $g^6$ . Kajantie *et al.* [17] evaluated perturbatively the last calculable contribution, that of order  $g^6 \ln(1/g^2)$ . This result is partly a conjecture, as this order receives a contribution from the complete  $\mathcal{O}(g^6)$  term. However, without going into the details, general arguments based on the pattern of singularity cancellation order by order can be given in order to make progress. The interested reader may consult the quoted reference for a discussion of these technical aspects. The pressure at order  $g^6 \ln(1/g^2)$  with  $N_f$  flavors is given by these authors as

$$\begin{aligned}
 P_6 = & \frac{8\pi^2}{45} T^4 \left(\frac{\alpha_s(M)}{\pi}\right)^3 \left\{ \left[ -659.2 - 65.89N_f - 7.653N_f^2 + 742.5 \left(1 + \frac{1}{6}N_f\right) \right. \right. \\
 & \left. \left. \times \left(1 - \frac{2}{33}N_f\right) \ln\left(\frac{M}{2\pi T}\right) \right] \ln\left[\frac{\alpha_s}{\pi} \left(1 + \frac{1}{6}N_f\right)\right] \right. \\
 & \left. - 475.6 \ln\left(\frac{\alpha_s}{\pi}\right) + q_a(N_f) \ln^2\left(\frac{M}{2\pi T}\right) + q_b(N_f) \ln\left(\frac{M}{2\pi T}\right) + q_c(N_f) \right\}
 \end{aligned}
 \tag{8.60}$$

where  $q_a(N_f), q_b(N_f), q_c(N_f)$  are polynomials in  $N_f$ . The polynomials  $q_{a,b}$  may be written down using the cancellation pattern alluded to earlier:

$$\begin{aligned}
 q_a(N_f) = & -\frac{1815}{16} \left(1 + \frac{5}{12}N_f\right) \left(1 - \frac{2}{33}N_f\right)^2 \\
 q_b(N_f) = & 2932.9 + 42.83N_f - 16.48N_f^2 + 0.2767N_f^3
 \end{aligned}
 \tag{8.61}$$

The last polynomial,  $q_c(N_f)$ , is the one that receives a nonperturbative contribution and is as yet uncalculated.

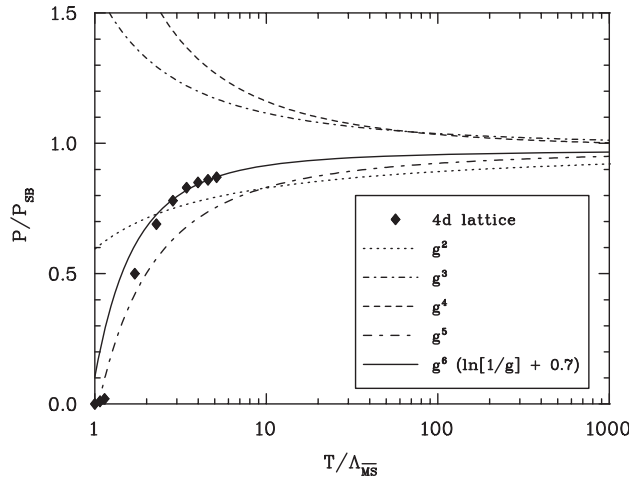


Fig. 8.1. Perturbative results for the pressure at various orders, including  $g^6$  with an optimal constant, normalized to the noninteracting Stefan–Boltzmann value  $P_{SB}$  (Kajantie *et al.* [17]), against the scaled temperature.

It is instructive to examine the convergence of the perturbative expansion term by term. This is shown in Figure 8.1 for the pure gluon case with  $N = 3$  and  $N_f = 0$ . The ratio of the pressure and its value in the Stefan–Boltzmann limit is plotted against the reduced temperature. At high temperatures, the pressure tends to the Stefan–Boltzmann limit.

### 8.5 Gluon propagator and linear response

In applying linear response theory to nonabelian gauge theories one must be careful to distinguish between gauge-invariant, physically observable, quantities and gauge-noninvariant quantities. The latter may still be relevant, though, provided that we can construct some observable out of them. This can be demonstrated with color electric screening.

The components of the color electric field,

$$E_i^a = F_{i0}^a = \partial_i A_0^a - \partial_0 A_i^a - g f^{abc} A_i^b A_0^c \tag{8.62}$$

are not gauge invariant, unlike the electric field of QED, which is gauge invariant. Thus color electric screening as a physical phenomenon cannot be demonstrated on the basis of the color electric field alone. However, screening can be examined by computing the free energy  $V$  of a static, color-singlet (total color charge zero), quark–antiquark pair as a function of separation  $R$ . This can be done most directly in the temporal axial gauge (TAG)  $A_0^a = 0$ , for in this gauge the electric field is

$$\mathbf{E}_a = -\frac{\partial \mathbf{A}_a}{\partial t} \quad \text{TAG} \tag{8.63}$$

Then the analysis of Section 6.3 can be applied, with the result that the static dielectric function is (cf. (6.64))

$$\epsilon(\mathbf{q}) = 1 + \frac{F(0, \mathbf{q})}{\mathbf{q}^2}, \quad \text{TAG} \quad (8.64)$$

The scalar function  $F$  must be computed in TAG. Referring to (6.58) and (8.46) (except that in the latter there is no ghost diagram) one finds that, for the pure TAG gluon contribution<sup>†</sup> [19],

$$\begin{aligned} \Pi_{00}^{\text{mat}}(q_0, q) &= -\frac{g^2 N}{4\pi^2} \int_0^\infty dk k N_B(k) \\ &\times \text{Re} \left[ 4 - \frac{(q^2 - 2kq_0 - q_0^2)(2k + q_0)^2}{2k^2(k + q_0)^2} + \frac{(2k + q_0)^2}{2kq} \right. \\ &\quad \left. + \left( 1 + \frac{(k^2 + (k + q_0)^2 - q^2)^2}{4k^2(k + q_0)^2} \right) \ln \left( \frac{R_+}{R_-} \right) \right] \quad (8.65) \end{aligned}$$

$$\begin{aligned} \Pi_{ii}^{\text{mat}}(q_0, q) &= -\frac{g^2 N}{4\pi^2} \int_0^\infty dk k N_B(k) \\ &\times \text{Re} \left[ 12 - \frac{2}{(k + q_0)^2} \left( 8k^2 - q^2 - \frac{q^4}{4k^2} + 9q_0(q_0 + 2k) \right. \right. \\ &\quad \left. \left. - \frac{5q^2}{4k^2}(q_0 + 2k)q_0 + \frac{3q_0^2}{2k^2}(q_0 + 2k)^2 \right) \right. \\ &\quad \left. + \frac{1}{2kq} \left\{ -q^2 + 10k^2 + 10(k + q_0)^2 \right. \right. \\ &\quad \left. \left. - \frac{1}{2k^2(k + q_0)^2} [k^2 + (k + q_0)^2 - q^2]^2 \right. \right. \\ &\quad \left. \left. \times [3k^2 + 3(k + q_0)^2 + \frac{1}{2}q^2] \right\} \ln \left( \frac{R_+}{R_-} \right) \right] \quad (8.66) \end{aligned}$$

where  $q = |\mathbf{q}|$ ,  $q_0 = 2\pi n T i$ ,  $R_\pm = q^2 - 2kq_0 - q_0^2 \pm 2kq$ , and  $\text{Re}$  means that the even part of the following function of  $q_0$  should be taken. The quark matter contributions are given by (5.51) with the substitution

<sup>†</sup> The axial-gauge pole  $1/(n \cdot p)$  can be handled in one-loop diagrams with the principal value ( $PV$ ) prescription. For example,

$$\text{P.V.} \frac{1}{n \cdot p} = \lim_{\epsilon \rightarrow 0} \frac{1}{2} \left( \frac{1}{n \cdot p + i\epsilon} + \frac{1}{n \cdot p - i\epsilon} \right)$$

see [18]. This makes sense in TAG at  $T > 0$  only after analytic continuation of  $p_0$  and replacement of frequency sums by contour integrals.

$e^2 \rightarrow \frac{1}{2}g^2$ . In the following discussion, we will need only the static limit of the vacuum contribution,

$$F^{\text{vac}}(0, q) = \frac{g^2}{48\pi^2} (11N - 2N_f) q^2 \ln \left( \frac{q^2}{M^2} \right) \quad \text{TAG} \quad (8.67)$$

Recall that  $\Pi^{\mu\nu}$  is related to  $F$  and  $G$  in TAG just as in (5.46).

Consider the vacuum dielectric function. Inserting (8.67) into (8.64), we obtain the vacuum-polarization-corrected effective charge

$$\begin{aligned} \bar{g}^2(q) &= \frac{g^2}{\epsilon(q)} = \frac{g^2}{1 + (g^2/48\pi^2)(11N - 2N_f) \ln(q^2/M^2)} \\ &= \frac{48\pi^2}{(11N - 2N_f) \ln(q^2/\Lambda^2)} \end{aligned} \quad (8.68)$$

which is the same as the renormalization-group charge.

The situation in other gauges is not so simple. Consider the set of covariant gauges (COVG). Then from (8.62) the color electric field has terms that are linear or quadratic in the vector potential. To find the linear response to an applied color electric field (such as that due to stationary quarks) we need to compute the correlation function between two electric field operators, and that entails knowledge of not only the propagator but also the three- and four-point gluon functions

$$\langle A_\mu A_\nu A_\alpha \rangle \quad \langle A_\mu A_\nu A_\sigma A_\gamma \rangle$$

There is also the complication of the ghost field. What happens if we neglect the nonlinearity in (8.62) and naively apply (8.64)? From (8.19) we have

$$F^{\text{vac}}(0, q) = \frac{g^2}{48\pi^2} \left[ \left( \frac{13}{12} - \frac{3}{2}\rho \right) N - 2N_f \right] q^2 \ln \left( \frac{q^2}{M^2} \right) \quad \text{COVG} \quad (8.69)$$

This does not yield the correct renormalization-group-improved charge, nor does it yield the correct vacuum-polarization-corrected potential between stationary quarks. This should be expected. In Section 8.2 we found that knowledge of the gluon propagator alone was not sufficient to determine the  $\beta$ -function in the covariant gauges, although it was sufficient in the axial gauges.

Computation of the free energy, as a function of separation, of the static quark–antiquark pair at  $T > 0$  (in TAG) proceeds just as in QED. At large separation,

$$V(R) = \frac{Q_1 \cdot Q_2}{4\pi} \frac{e^{-m_{\text{el}}R}}{R} \quad (8.70)$$

In the color-singlet state, the product of charges is  $Q_1 \cdot Q_2 = -g^2 N_g / 2N$ . Since (8.70) is physically measurable (at least in principle!),  $m_{\text{el}}$  must be gauge invariant. In TAG, it is given by

$$m_{\text{el}}^2 = F(0, \mathbf{q} \rightarrow 0) \quad \text{TAG} \quad (8.71)$$

which is an exact relation.

To one-loop order, all gauges receive the same contribution to  $\Pi^{\mu\nu}$  from dynamical quarks. To focus on the essentials, we shall consider a quark-free world in the remainder of this section.

In the Feynman gauge (FG,  $\rho = 1$ ), the  $T > 0$  contribution to the gluon self-energy is

$$\begin{aligned} \Pi_{00}^{\text{mat}}(q_0, q) &= -\frac{g^2 N}{4\pi^2} \int_0^\infty dk k N_B(k) \\ &\quad \times \text{Re} \left\{ 4 + \frac{1}{qk} [(q_0 + 2k)^2 - 2q^2] \ln \left( \frac{R_+}{R_-} \right) \right\} \end{aligned} \quad (8.72)$$

$$\begin{aligned} \Pi_{ii}^{\text{mat}}(q_0, q) &= \frac{g^2 N}{4\pi^2} \int_0^\infty dk k N_B(k) \\ &\quad \times \text{Re} \left[ 4 + \frac{1}{qk} (4q_0^2 - 4kq_0 - 4k^2 - 3q^2) \ln \left( \frac{R_+}{R_-} \right) \right] \end{aligned} \quad (8.73)$$

These are not the same as (8.65) and (8.66). Thus  $\Pi^{\mu\nu}$ , and the functions  $F$  and  $G$ , are not gauge invariant in nonabelian gauge theories.

From the perspective of screening, the interesting limit is  $q_0 = 0$ ,  $|\mathbf{q}| = q \rightarrow 0$ . One finds that in TAG

$$\begin{aligned} F(0, q \rightarrow 0) &= -\Pi_{00}(0, q \rightarrow 0) \\ &= \frac{1}{3}g^2 NT^2 - \frac{1}{4}g^2 NTq - \frac{11}{48} \frac{g^2}{\pi^2} Nq^2 \ln \left( \frac{q^2}{T^2} \right) + \dots \end{aligned} \quad (8.74)$$

$$G(0, q \rightarrow 0) = \frac{1}{2}\Pi_{ii}(0, q \rightarrow 0) = -\frac{5}{16}g^2 NTq + \dots \quad (8.75)$$

and in FG

$$F(0, q \rightarrow 0) = -\Pi_{00}(0, q \rightarrow 0) = \frac{1}{3}g^2 NT^2 - \frac{1}{4}g^2 NTq + \dots \quad (8.76)$$

$$G(0, q \rightarrow 0) = \frac{1}{2}\Pi_{ii}(0, q \rightarrow 0) = -\frac{3}{16}g^2 NTq + \dots \quad (8.77)$$

There are a number of interesting aspects to these results. The first two terms of (8.74) and (8.76) are identical. This would not have been expected on the basis of our earlier discussion of electric screening. The reason that they are, and must be, the same is that these first two terms of  $F$  give rise to the order  $g^3$  and order  $g^4 \ln g^2$  terms in the pressure via summation of the ring diagrams (recall Section 6.5). The coefficients of all terms in

the pressure up to (but not including)  $g^4$  must be gauge independent, on account of (8.55). The third term of (8.74) combines with the vacuum contribution to yield

$$\frac{11}{48} \frac{g^2}{\pi^2} N q^2 \ln \left( \frac{T^2}{M^2} \right)$$

So again we see that we should choose  $M$  proportional to  $T$  to eliminate potentially large logarithms at high temperature. The first nonzero term of  $G$  is gauge dependent. This will be discussed further in Section 8.7.

Plasma oscillations may be discussed in a manner parallel to the discussion in Section 6.6. In TAG, a physical gauge with the proper number of gluon-polarization degrees of freedom and no ghosts, one finds that the long-wavelength dispersion relations for transverse and longitudinal oscillations are

$$\begin{aligned} \omega_T^2 &= \omega_P^2 + \frac{6}{5} k^2 + \dots \\ \omega_L^2 &= \omega_P^2 + \frac{3}{5} k^2 + \dots \end{aligned} \tag{8.78}$$

where  $\omega_P^2 = g^2 NT^2/9$ . These waves are damped with damping constant  $\gamma_T = \gamma_L = g^2 NT/24\pi$ . The short-wavelength longitudinal oscillations are overdamped and do not propagate. The transverse oscillations have the spectrum

$$\omega_T^2 = k^2 + \frac{3}{2} \omega_P^2 + \dots \tag{8.79}$$

and to order  $g^2$  are not damped by thermal effects.

A proper linear response analysis has also been done in another gauge, the Coulomb gauge [20]. The results are identical to (8.78) and (8.79). If one tries to do a cheap analysis in an unphysical gauge by simply searching for the poles of the gluon propagator, one obtains certain erroneous results. For example, in the Feynman gauge one recovers (8.78) and (8.79), but the damping constant is a factor 5 too large and of the opposite (wrong) sign. In addition, short-wavelength longitudinal waves propagate with  $\omega_L^2 = k^2 + \dots$ , which is unphysical.

It must be acknowledged that, at this time, color plasma waves are an enigma. Whether they represent physically observable phenomena has not been rigorously established.

## 8.6 Instantons

Instantons are nonperturbative solutions of the classical field equations which carry topological charge. After their discovery by Belavin *et al.*

[21] it was hoped that they would provide a means of understanding confinement. That has turned out not to be the case. In QCD their effects are reliably computed only at short distance (or high temperature). In this domain, it has been found that they are always dominated by perturbative corrections. For this reason, and because the mathematics of instantons can become quite involved, this brief section will present only an overview.

Instantons contribute to the partition function *in addition* to all perturbative contributions. Although not quantitatively important in their own right, these nonperturbative solutions are of course interesting in principle. They have also been used in a more phenomenological way to understand various aspects of chiral symmetry breaking and restoration and hadronic structure.

Consider an SU(2) gauge field theory without quarks. It is advantageous in this context to work in Euclidean space, with Greek indices running from 1 to 4. Define the matrix functions

$$\begin{aligned} A_\mu &= -ig\left(\frac{1}{2}\sigma^a\right)A_\mu^a \\ F_{\mu\nu} &= -ig\left(\frac{1}{2}\sigma^a\right)F_{\mu\nu}^a \end{aligned} \quad (8.80)$$

The action is

$$S = \frac{1}{2g^2} \int d^4x \operatorname{Tr}(F_{\mu\nu}F^{\mu\nu}) \quad (8.81)$$

and the classical equations of motion are

$$\partial^\mu F_{\mu\nu} + [A^\mu, F_{\mu\nu}] = 0 \quad (8.82)$$

We make the ansatz that

$$A_\mu = i\bar{\sigma}_{\mu\nu}a^\nu \quad (8.83)$$

where  $a^\nu$  is spacetime dependent, and we define the following objects:

$$\begin{aligned} \sigma_{ij} &= -i\left[\frac{1}{2}\sigma_i, \frac{1}{2}\sigma_j\right] \\ \sigma_{i4} &= \frac{1}{2}\sigma_i \\ \sigma_{\mu\nu} &= -\sigma_{\nu\mu} \\ \bar{\sigma}_{ij} &= \sigma_{ij} \\ \bar{\sigma}_{i4} &= -\sigma_{i4} \end{aligned} \quad (8.84)$$

With a dual defined by

$$*\sigma_{\mu\nu} = \frac{1}{2}\epsilon_{\mu\nu\alpha\beta}\sigma^{\alpha\beta}$$

we find that

$$\begin{aligned} {}^*\sigma_{\mu\nu} &= \sigma_{\mu\nu} && \text{self-dual} \\ {}^*\bar{\sigma}_{\mu\nu} &= -\bar{\sigma}_{\mu\nu} && \text{antiself-dual} \end{aligned} \quad (8.85)$$

The equations of motion are satisfied when

$$\begin{aligned} a_\mu &= \partial_\mu \ln \phi \\ \partial^2 \phi &= 0 \end{aligned} \quad (8.86)$$

This solution is said to be self-dual because  ${}^*F_{\mu\nu} = F_{\mu\nu}$ . An antiself-dual solution (with  ${}^*F_{\mu\nu} = -F_{\mu\nu}$ ) is obtained with

$$A_\mu = i\sigma_{\mu\nu}a^\nu \quad (8.87)$$

In both cases the classical action can be expressed as

$$S = \frac{1}{2g^2} \int d^4x \partial^2 \partial^2 \ln \phi \quad (8.88)$$

For the solution of Laplace's equation we have

$$\phi(x) = 1 + \sum_{i=1}^n \frac{\lambda_i^2}{(x - y_i)^2} \quad (8.89)$$

where each  $\lambda_i$  is a real number and each  $y_i$  is a fixed vector. Clearly  $y_i$  represents the position of some object and  $\lambda_i$  its size. When this solution is used in the self-dual ansatz, it is said to represent  $n$  instantons; when it is used in the antiself-dual ansatz it is said to represent  $n$  anti-instantons. The instantons and anti-instantons represent tunnelings between different states.

These field configurations can be characterized by a topological charge  $q$ , a gauge invariant, called a Pontryagin index:

$$q = \frac{1}{16\pi^2} \int d^4x \operatorname{Tr} ({}^*F_{\mu\nu} F^{\mu\nu}) \quad (8.90)$$

A direct calculation shows that  $q = n$  for the  $n$ -instanton solution and  $q = -n$  for the  $n$ -anti-instanton solution. There is no known exact solution for  $n$  instantons and  $n'$  anti-instantons. It is not possible to change the Pontryagin index by a smooth deformation of the gauge field. Since perturbative calculations always start with  $A_\mu = 0$  and  $q = 0$ , the instantons and anti-instantons make topologically distinct contributions to the functional integral.

When computing the partition function at  $T = 0$  (useful for calculating vacuum correlation functions), the most straightforward approach is to treat the instantons and anti-instantons as individual, noninteracting objects (the dilute gas approximation, DGA). Only instantons with  $q = 1$



and anti-instantons with  $q = -1$  are included. One-loop quantum corrections can be included by writing

$$A_\mu = A_\mu^{\text{cl}} + A'_\mu$$

where  $A_\mu^{\text{cl}}$  is the classical solution, expanding the Lagrangian in powers of  $A'_\mu$  and dropping terms cubic and quartic in  $A'_\mu$ . That is, the quantum fluctuations must be calculated in the presence of a background instanton (or anti-instanton) field. For  $SU(N)$ , the  $SU(2)$  instantons must be embedded in the appropriate fashion. The calculations of t'Hooft [22], in particular, are a *tour de force* of mathematical physics. The result is simple and elegant. It is (assuming no state mixing)

$$\ln Z_{\text{DGA}} = 2C_N V \beta \int_0^\infty \frac{d\lambda}{\lambda^5} \left( \frac{4\pi^2}{g^2} \right)^{2N} \exp\left(-\frac{8\pi^2}{\bar{g}^2}\right) \quad (8.91)$$

We make the following remarks.

- 1 The exponential of the classical action is evident.
- 2 The factor  $V\beta$  is the total spacetime volume.
- 3 The factor 2 arises because both instantons and anti-instantons are included.
- 4 The factor  $C_N$  is group-theoretic in origin. In the Pauli–Villars regularization scheme,

$$C_N = \frac{4}{\pi^2} \frac{\exp[-0.433 - 0.292(N - 2 - N_f)]}{(N - 1)!(N - 2)!} \quad (8.92)$$

- 5 Integration over scale size  $\lambda$  must be done. The power  $-5$  of  $\lambda$  arises from the scale size and from the four components of the position coordinate. It also is required so that  $\ln Z$  is dimensionless.
- 6 Quantum fluctuations amount to replacing the coupling constant  $g^2$  with the renormalization-group running coupling

$$\bar{g}^2 = \frac{24\pi^2}{(11N - 2N_f) \ln(1/\lambda\Lambda_R)} \quad (8.93)$$

in the exponential factor, although this replacement is presumed to happen (at the next order) in the pre-exponential factor as well. Here  $\Lambda_R$  is the QCD scale parameter in the Pauli–Villars scheme.

- 7 There should be an additional factor in  $\ln Z_{\text{DGA}}$ , which is

$$\prod_f (m_f \lambda)$$

for each light quark ( $m_f < \lambda^{-1}$ ) flavor. Light quarks greatly suppress instantons.

8 The integral over  $\lambda$  does not exist: it diverges for large  $\lambda$ . Thus one must go beyond the dilute gas approximation in the QCD vacuum and confront the infrared confinement problem.

The way to avoid point 8 is to focus on a physical circumstance which provides a natural cutoff on instanton size  $\lambda$ . For example, we could consider computing instanton-induced corrections to the process  $e^+e^- \rightarrow$  hadron jets at high energy. A cutoff would then be supplied by the center-of-mass energy  $\sqrt{s}$ ; the dominant contribution should come from instanton scale sizes  $\lambda \approx 1/\sqrt{s}$ . Another circumstance, of interest to us, is the contribution of instantons to the thermodynamic potential of a high-temperature quark–gluon plasma. At high temperatures, color electric fields should be screened just as in QED plasma. The temperature should provide an infrared cutoff on instanton sizes.

It is possible to generalize these solutions to finite temperature. We still work in Euclidean space but  $x_4$  is replaced by the variable  $\tau$ . The instanton solutions must now be periodic in  $\tau$  with period  $\beta$ . This is accomplished by making the field  $\phi$  periodic [23]. The  $n = 1$  solution goes over into

$$\begin{aligned} \phi &= 1 + \lambda^2 \sum_{k=-\infty}^{\infty} [(\mathbf{x} - \mathbf{y}_1)^2 + (\tau - \tau_1 - k\beta)^2]^{-1} \\ &= 1 + \frac{\pi T \lambda^2}{|\mathbf{x} - \mathbf{y}_1|} \frac{\sinh(2\pi T |\mathbf{x} - \mathbf{y}_1|)}{\cosh(2\pi T |\mathbf{x} - \mathbf{y}_1|) - \cos[2\pi T (\tau - \tau_1)]} \end{aligned} \quad (8.94)$$

Here,  $\mathbf{y}_1$  and  $0 \leq \tau_1 \leq \beta$  represent the position of the instanton, while the summation over  $k$  replicates it periodically along the imaginary time axis. Surprisingly, the finite-temperature instanton and anti-instanton have exactly the same classical action,  $8\pi^2/g^2$ , as the  $T = 0$  instanton and anti-instanton.

It is necessary to compute the one-loop quantum correction in the background field of an instanton or anti-instanton at finite temperature. This is a formidable task but has been done by Pisarski and Yaffe [24]. The result is that the integrand in (8.91) is multiplied by a cutoff factor

$$\exp\left[-\frac{1}{3}(2N + N_f)\pi^2 T^2 \lambda^2\right] \quad (8.95)$$

at large  $\lambda$ . This means that the  $\lambda$  integration is now both infrared and ultraviolet convergent. Finite temperature suppresses large instantons as expected. The lack of appearance of the coupling constant in the cutoff is simply understood as follows. At  $T = 0$ , quantum corrections replace the coupling constant in the classical action with the renormalization-group running coupling. Therefore we may postulate that at finite temperature

the running coupling would be replaced by the static screened charge

$$\frac{8\pi^2}{\bar{g}^2} = \frac{8\pi^2}{g^2} + \left( \frac{11N}{6} - \frac{N_f}{3} \right) \ln \left( \frac{\mathbf{q}^2}{M^2} \right) + \frac{8\pi^2 m_{\text{el}}^2}{g^2 \mathbf{q}^2} \quad (8.96)$$

where  $m_{\text{el}}^2$  is given by (8.49). The screening factor (8.95) is reproduced by the  $m_{\text{el}}^2/g^2$  term in (8.96) if we make the replacement  $\mathbf{q}^2 \rightarrow 4/\lambda^2$ .

Instanton effects are greatest in a world without light quarks, on account of point 7 above. Then the contribution to the pressure is

$$P_{\text{DGA}} = 2C_N \int_0^\infty \frac{d\lambda}{\lambda^5} \left( \frac{4\pi^2}{\bar{g}^2} \right)^{2N} \exp \left( -\frac{8\pi^2}{\bar{g}^2} - \frac{2}{3} N (\pi T \lambda)^2 \right) \quad (8.97)$$

which can be integrated to give

$$P_{\text{DGA}} = T^4 \left( \frac{\Lambda_R}{T} \right)^{11N/3} \sum_{l=0}^{2N} a_l(N) \left[ \ln \left( \frac{T}{\Lambda_R} \right) \right]^l \quad (8.98)$$

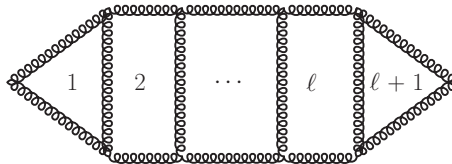
The coefficients  $a_l(N)$  depend on  $N$  and must be computed numerically. The most noteworthy feature of  $P_{\text{DGA}}$  is that it decreases dramatically with increasing temperature. For instance, for SU(3) it falls as  $\Lambda_R^{11}/T^7$ , modulo logarithms. Comparison of these results with the perturbation theory results is left as an exercise.

Extensive numerical studies have been performed of an instanton-liquid description of QCD at zero and finite temperature. The reader is referred to the review of Schäfer and Shuryak [25].

## 8.7 Infrared problems

It would seem that if only we had the strength and willpower, we could continue to calculate corrections to  $P$  and  $\Pi^{\mu\nu}$  to arbitrary order in  $g$ . However, a barrier that arises at order  $g^6$  for  $P$  and at order  $g^4$  for  $\Pi^{\mu\nu}$  was identified by Lindé [26].

Let us investigate the infrared convergence of the  $(l+1)$ -loop diagram ( $l > 0$ )



There are  $2l$  three-gluon vertices and  $3l$  propagators. The dominant infrared behavior arises from the  $n = 0$  mode sums. To estimate, we dispense with the complicated tensorial structure of the propagator and the

vertex and write

$$g^{2l} \left( T \int d^3p \right)^{l+1} p^{2l} (p^2 + m^2)^{-3l} \tag{8.99}$$

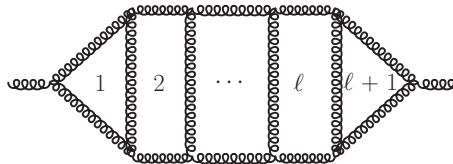
The first and third factors arise from the vertices, the second factor from the loop integration, and the last factor from the propagators. We have introduced a possible static infrared cutoff  $m$ . We may wish to identify  $m$  with the “electric mass”  $m_{\text{el}}^2 = F(0, \mathbf{0})$  or with the “magnetic mass”  $m_{\text{mag}}^2 = G(0, \mathbf{0})$ . In any case, (8.99) is of order

$$\begin{aligned} g^{2l} T^4 & \quad \text{for } l = 1, 2 \\ g^6 T^4 \ln(T/m) & \quad \text{for } l = 3 \\ g^6 T^4 (g^2 T/m)^{l-3} & \quad \text{for } l > 3 \end{aligned} \tag{8.100}$$

We have placed an ultraviolet cutoff  $T$  on the momentum integration. This cutoff should arise automatically when summing over all modes  $n$ .

The interesting aspect of (8.100) is that if  $m = 0$  and  $l > 2$ , then the diagram is infrared divergent. Now it may happen that when all diagrams of the same order are added together the coefficients of the infrared divergent parts are zero, although there is no symmetry to suggest that this is the case. The possibility is difficult to verify or deny, owing to the complexity of the diagrams. If we take  $m = m_{\text{el}} \sim gT$  then no problem arises. At one-loop order,  $m_{\text{mag}}$  vanishes in all gauges; the next possibility is that  $m_{\text{mag}} \sim g^2 T$ . Substitution in (8.100) then suggests that all loops with  $l > 3$  contribute to order  $g^6$ ! It is not known how to sum all such diagrams, thus making it impractical even in principle to calculate analytically the coefficient of the order- $g^6$  term in  $P$ .

The same difficulty arises if we attempt to compute the static infrared limit of the gluon self-energy. For example, the diagram



at  $q_0 = 0, \mathbf{q} \rightarrow \mathbf{0}$  is of order

$$\begin{aligned} g^4 T^2 \ln(T/m) & \quad \text{for } l = 1 \\ g^4 T^2 (g^2 T/m)^{l-1} & \quad \text{for } l > 1 \end{aligned} \tag{8.101}$$

So, the infrared problem arises for  $\Pi^{\mu\nu}$  at order  $g^4$ . Suppose, for the purpose of illustration, that  $m_{\text{mag}}^2 = cg^4 T^2$ . Then (8.101) suggests that to compute  $c$  we must sum an infinite set of diagrams. The constant  $c$  would then arise self-consistently. The magnetic contribution to the sum of ring

diagrams would be proportional to  $m_{\text{mag}}^3 T \sim g^6 T^4$ . This is another way of viewing the qualitatively different infrared effects that may arise at order  $g^6$  in the pressure.

The static infrared problem in the above diagrams occurs when the momentum  $p \leq g^2 T$ . Another way to see this is to examine the factor  $[p^2 + G(0, p)]^{-1}$  in the propagator. This changes sign as  $p \rightarrow 0$ ; in TAG,  $G(0, p) \rightarrow -(5/16)g^2 NTp$  and for the case of an arbitrary COVG,  $G(0, p) \rightarrow -\{[8 + (\rho + 1)^2]/64\}g^2 NTp$ .

The resolution of this problem, as suggested by Braaten [27], involves effective-field-theory methods coupled with lattice gauge calculations. However, it probably does not have much quantitative impact on thermodynamic functions like  $P$  at extremely high temperatures since it first occurs at order  $g^6$  and  $g(T) \rightarrow 0$  as  $T \rightarrow \infty$ .

### 8.8 Strange quark matter

Strange particles, like kaons and hyperons, do not play any role in daily life; that is to say, they are not stable particles and they are not found in atomic nuclei. Generally, they are only produced in high-energy reactions, and subsequently decay into nonstrange particles via the weak interactions. Could the situation be different in cold and dense quark matter? For cold neutron matter the baryon density is approximately

$$n = 2 \int \frac{d^3 p}{(2\pi)^3} \theta(p_F - p) = \frac{p_F^3}{3\pi^2} \quad (8.102)$$

where the Fermi momentum is  $p_F^2 = \mu^2 - m_N^2$ . One may estimate the density at which neutrons overlap in coordinate space by multiplying this density by the volume of a nucleon, taking the nucleon radius to be 0.8 fm. Although very crude, this estimate determines the critical chemical potential as 1050 MeV, where a qualitative change in the nature of hadronic matter ought to occur. Since each quark carries one-third of a baryon charge, the quark chemical potential would be 350 MeV. This is larger than the generally accepted strange quark mass (see Table 8.2) and so allows for the possibility of the existence of strange quarks even when  $T = 0$ . Strange quarks might be produced and eventually come to equilibrium via the weak interactions  $d \leftrightarrow u + e + \bar{\nu}_e$ ,  $s \leftrightarrow u + e + \bar{\nu}_e$ , and  $s + u \leftrightarrow u + d$ , provided that the circumstances are right. Indeed, it may very well be energetically favorable for some  $u$  and  $d$  quarks to be converted into  $s$  quarks at high density. The situation would be analogous to the presence of neutrons in nuclei. In free space, a neutron decays weakly into a proton, an electron, and an antineutrino. That does not happen in radioactively stable nuclei or in nuclear matter, because the

Pauli exclusion principle forbids the addition of a proton with an energy below the Fermi energy.

Let us assume chemical equilibrium under the weak interactions among  $u$ ,  $d$ ,  $s$  quarks and electrons. Then the aforementioned reactions imply that

$$\mu_u + \mu_e = \mu_d = \mu_s \quad (8.103)$$

For the present discussion the neutrinos may be neglected. We require that bulk matter be electrically neutral. Then we have the constraint

$$\frac{2}{3}n_u - \frac{1}{3}n_d - \frac{1}{3}n_s - n_e = 0 \quad (8.104)$$

The densities are functions of the chemical potentials. Together, (8.103) and (8.104) allow only one independent chemical potential.

For simplicity, first analyze the thermodynamics neglecting perturbative interactions among the quarks. For the large chemical potentials of interest it is reasonable to set  $m_e = m_u = m_d = 0$ . However,  $m_s$  is not so small and must be kept nonzero. The thermodynamic potential is a sum of contributions from each species:

$$\begin{aligned} \Omega_e &= -\frac{\mu_e^4}{12\pi^2} & \Omega_u &= -\frac{\mu_u^4}{4\pi^2} & \Omega_d &= -\frac{\mu_d^4}{4\pi^2} \\ \Omega_s &= -\frac{1}{4\pi^2} \left[ \mu_s \sqrt{\mu_s^2 - m_s^2} (\mu_s^2 - 2.5m_s^2) \right. \\ &\quad \left. + 1.5m_s^4 \ln \left( \frac{\mu_s + \sqrt{\mu_s^2 - m_s^2}}{m_s} \right) \right] \end{aligned} \quad (8.105)$$

The energy density carried by the fermions is added to that associated with the vacuum, sometimes referred to as the MIT bag model constant,  $B$ , yielding a total energy density

$$\epsilon = \sum_i (\Omega_i + \mu_i n_i) + B \quad (8.106)$$

The baryon number density is

$$n_B = \frac{1}{3}(n_u + n_d + n_s) \quad (8.107)$$

The quark matter is in stable mechanical equilibrium when  $P = 0$ . Including the bag pressure, this means

$$P = \sum_i P_i - B = -\sum_i \Omega_i - B = 0 \quad (8.108)$$

With the set of equations above, all parameters can be calculated for a given choice of  $m_s$  and  $B$ . The result of such calculations is shown in Figure 8.2.

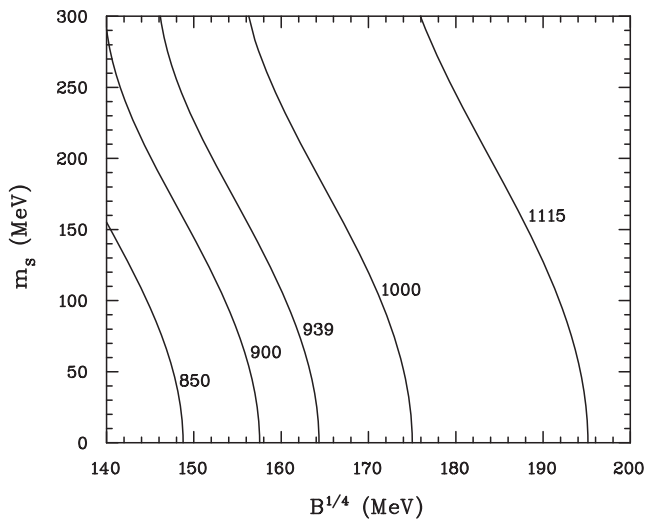


Fig. 8.2. Contours of fixed energy per baryon (in MeV) for strange quark matter in the  $B^{1/4}-m_s$  plane;  $B$  is the bag model constant.

It is known that nonstrange quark matter is unbound. It must have an energy per baryon of at least  $930 \text{ MeV} + \Delta$  in order that ordinary atomic nuclei do not decay into nonstrange quark matter, which has never been observed. A detailed calculation suggests  $\Delta = 4 \text{ MeV}$  [28]. A straightforward calculation then leads to a minimum value  $B_{\text{min}} = (145 \text{ MeV})^4$ : this is the minimum value of the bag constant needed for atomic nuclei to be stable (in the  $T = 0$  case, and neglecting interaction between the quarks). Considering Figure 8.2, normal atomic nuclei do not exist for values of  $B < B_{\text{min}}$ . To the left of the 939 MeV contour, strange quark matter would be stable against decay into nucleons. The analysis outlined above is for degenerate, noninteracting, quark matter in bulk. Calculations including exchange corrections to order  $\alpha_s$  have also been done. Farhi and Jaffe [28] found that the inclusion of exchange interactions up to order  $\alpha_s$  effectively lowers  $B_{\text{min}}$  to smaller values.

The question arises of why ordinary nuclei have not decayed into strange quark matter, if it is more stable? The answer is that the conversion of many  $u$  and  $d$  quarks into  $s$  quarks requires a very high order of the weak interaction; thus the probability for this to happen is essentially zero. It is for this reason that nuclei may have been mistakenly taken to be the ground state of hadronic matter. Searches for strange quark matter in terrestrial experiments and in astrophysical observations have been ongoing. The effects of finite temperature and of finite size on the stability have been evaluated [29]. The fact that strange matter might be self-bound is in itself a fascinating proposition. The theoretical uncertainties

surrounding it will surely decrease as our ability to perform numerical lattice gauge calculations at finite density grows.

### 8.9 Color superconductivity

The experimental discovery of superconductivity by Kamerlingh Onnes in 1911 was totally unexpected. It defied fundamental theoretical understanding until the Nobel-prize-winning work of Bardeen, Cooper, and Schrieffer (BCS) in 1957. The discovery of high- $T_c$  materials in 1986 was also totally unexpected; its theoretical understanding is still a topic of research. Superconductivity has many applications nowadays, primarily in magnets used in research and in medicine. Conventional superconductivity arises from the pairing of electrons with equal but nearly opposite momentum near the Fermi surface. This pairing occurs because of a very weak attraction originating in phonon exchange, despite the fact that electrons experience a repulsive Coulomb interaction. This is one of the reasons why it took so long to work out a fundamental theoretical description of superconductivity. In QCD the situation is different. In a cold quark gas, single-gluon exchange is attractive for two quarks in a state that is antisymmetric in color, the  $\bar{3}$  channel. The possibility of color superconductivity therefore exists, and indeed it happens.

Color superconductivity was first studied by Barrois [30] and Frautschi [31]. Further studies were reported by Bailin and Love [32], but it was not until 1998 that the field exploded in a flood of research papers led by Alford, Rajagopal, and Wilczek [33], and Rapp *et al.* [34]. These studies can be categorized into one of two classes: weak coupling methods using the fundamental QCD Lagrangian, valid at asymptotically high densities; and phenomenological methods using four-quark interactions, some motivated by instantons, which are intended for application at densities not much greater than those in ordinary atomic nuclei.

In order to allow for the pairing of quarks, we follow the path pioneered by Nambu and by Gorkov [35]. An eight-component Dirac field is introduced as

$$\Psi = (\psi, \bar{\psi}_T)$$

where T denotes the transpose. The inverse propagator is an  $8 \times 8$  matrix in Dirac space:

$$\mathcal{G}^{-1}(p) = \mathcal{G}_0^{-1}(p) + \Sigma(p) = \begin{pmatrix} \not{p} - m + \mu\gamma_0 & \bar{\Delta} \\ \Delta & (\not{p} + m - \mu\gamma_0)_T \end{pmatrix} \quad (8.109)$$

Here  $\bar{\Delta} = \gamma_0 \Delta^\dagger \gamma_0$  and  $\Delta$  is an object with color, flavor, and Dirac indices, which have been suppressed. Setting  $\Delta = 0$  yields the free propagator for this eight-component field. The self-energy contribution to the block



diagonal components is neglected in order to focus on the coupling term, which gives rise to a gap and to superconductivity. In this section the chemical potential is separated out explicitly and is not subsumed into  $p_0$ .

In order to demonstrate the existence of superconductivity at high density we first focus on two flavors of massless  $u$  and  $d$  quarks with common chemical potential  $\mu$ . This is referred to as the 2SC phase. The assumptions that are usually made are: (i) the gap matrix is antisymmetric in both flavor and color, which is the channel in which single-gluon exchange is attractive; (ii) condensation occurs in the channel with zero angular momentum,  $J = 0$ ; (iii) the gap has positive parity, which is favored by the relatively weak instanton-induced interactions; (iv) chiral symmetry-breaking condensates coupling left- and right-handed quarks are neglected. Given these assumptions, the gap matrix takes the form

$$\Delta_{ij}^{ab}(p) = (\lambda_2)^{ab} (\tau_2)_{ij} C \gamma_5 [\Delta_+(p)P_+(p) + \Delta_-(p)P_-(p)] \quad (8.110)$$

where  $C = i\gamma^0\gamma^2$  is essentially the charge conjugation operator and makes the operand into a scalar rather than a pseudoscalar;  $a, b$  are color indices,  $i, j$  are flavor indices, and Dirac indices are suppressed. The operators  $P_+$  and  $P_-$  project onto particles and antiparticles, respectively:

$$P_{\pm}(p) = \frac{1}{2}(1 \pm \gamma_0\boldsymbol{\gamma} \cdot \hat{\mathbf{p}}) \quad (8.111)$$

Thus  $\Delta_+$  describes the modification of the propagator due to particle-particle pairing, whereas  $\Delta_-$  describes that due to antiparticle-antiparticle pairing. Particles and antiparticles are in this situation distinguished by the sign of the chemical potential.

The self-energy satisfies the Schwinger–Dyson equation,

$$\Sigma(k) = -g^2T \sum_n \int \frac{d^3p}{(2\pi)^3} \Gamma_{\mu}^a(k, p) \mathcal{G}(p) \Gamma_{\nu}^b(k, p) \mathcal{D}_{ab}^{\mu\nu}(k - p) \quad (8.112)$$

which is written in Minkowski space; the factor  $\Gamma_{\mu}^a(k, p)$  comes from the fully dressed quark–gluon vertex. At very high densities, where the running coupling becomes arbitrarily small,  $\Gamma_{\mu}^a(k, p)$  can be replaced by the bare vertex:

$$\Gamma_{\mu}^a = - \begin{pmatrix} \frac{1}{2}\lambda^a\gamma_{\mu} & 0 \\ 0 & -(\frac{1}{2}\lambda^a\gamma_{\mu})_{\text{T}} \end{pmatrix} \quad (8.113)$$

Then the Schwinger–Dyson equation determines the gap function:

$$\Delta(k) = g^2T \sum_n \int \frac{d^3p}{(2\pi)^3} \left( \gamma_{\mu} \frac{\lambda^a}{2} \right)_{\text{T}} \mathcal{G}_{21}(p) \left( \gamma_{\nu} \frac{\lambda^a}{2} \right) \mathcal{D}^{\mu\nu}(k - p) \quad (8.114)$$

The 2, 1 component of the quark propagator has entered here. With the given ansatz for the gap matrix, (8.110), we get

$$\mathcal{G}_{21}(p) = -\lambda_2 \tau_2 C \gamma_5 \left[ \frac{\Delta_+(p)P_-(p)}{p_0^2 - (|\mathbf{p}| - \mu)^2 - \Delta_+^2(p)} + \frac{\Delta_-(p)P_+(p)}{p_0^2 - (|\mathbf{p}| + \mu)^2 - \Delta_-^2(p)} \right] \tag{8.115}$$

The flavor factor  $\tau_2$  cancels on both sides of the gap equation; so does the color factor  $\lambda_2$ , because

$$\left(\frac{1}{2}\lambda^a\right)_T \lambda_2 \left(\frac{1}{2}\lambda^a\right) = -\frac{N+1}{2N}\lambda_2$$

After substitution one finds a pair of coupled gap equations,

$$\begin{aligned} \Delta_{\pm}(k) = & -\frac{g^2}{3}T \sum_n \int \frac{d^3p}{(2\pi)^3} \mathcal{D}^{\mu\nu}(k-p) \\ & \times \left\{ \text{Tr} [\gamma_{\mu}P_-(p)\gamma_{\nu}P_{\pm}(k)] \frac{\Delta_+(p)}{p_0^2 - (|\mathbf{p}| - \mu)^2 - \Delta_+^2(p)} \right. \\ & \left. + \text{Tr} [\gamma_{\mu}P_+(p)\gamma_{\nu}P_{\mp}(k)] \frac{\Delta_-(p)}{p_0^2 - (|\mathbf{p}| + \mu)^2 - \Delta_-^2(p)} \right\} \end{aligned} \tag{8.116}$$

to be solved for the gaps  $\Delta_{\pm}$ . In order to take into account static or dynamic screening of the color fields, the one-loop dressed gluon propagator in a covariant gauge is used, as given in Section 8.5.

For the scattering of quarks near the Fermi surface, which is relevant for determining the gaps, the energy transfer is negligible compared with the momentum transfer. With  $q \equiv k - p$ , this means that  $|q_0| \ll |\mathbf{q}|$ . Then  $q_0$  may be taken to zero wherever possible in the numerators of the gap equations, but not in the denominators since there may be a near singularity in the infrared. The Landau- and Coulomb-gauge gluon propagators give the same answer in this limit:

$$\begin{aligned} \Delta_{\pm}(k) = & \frac{g^2}{3}T \sum_n \int \frac{d^3p}{(2\pi)^3} \\ & \times \left\{ \frac{\Delta_{\pm}(p)}{p_0^2 - (|\mathbf{p}| \mp \mu)^2 - \Delta_{\pm}^2(p)} \left( \frac{3 - \hat{\mathbf{k}} \cdot \hat{\mathbf{p}}}{q^2 - G(q)} + \frac{1 + \hat{\mathbf{k}} \cdot \hat{\mathbf{p}}}{q^2 - F(q)} \right) \right. \\ & \left. + \frac{\Delta_{\mp}(p)}{p_0^2 - (|\mathbf{p}| \pm \mu)^2 - \Delta_{\mp}^2(p)} \left( \frac{1 + \hat{\mathbf{k}} \cdot \hat{\mathbf{p}}}{q^2 - G(q)} + \frac{1 - \hat{\mathbf{k}} \cdot \hat{\mathbf{p}}}{q^2 - F(q)} \right) \right\} \end{aligned} \tag{8.117}$$

These gaps are gauge independent only in this kinematic limit. This is a consequence of the fact that the gaps are determined by the scattering of quarks that are almost on-shell. Of course, any physical observable must be gauge independent. If one is working to higher order in the interactions, the approximations made above would not be acceptable.

Only the first term in the gap equation has a singularity on the Fermi surface, and so we keep it but drop the second term. This gives rise to a single integral equation to be solved for  $\Delta \equiv \Delta_+$ , the gap for quasi-particles and their holes near the Fermi surface (we are not interested in the gap for the antiparticles). In order to solve the integral equation for the gap we make a further physically motivated approximation. Since the participating quarks are those on or very near the Fermi surface, they all have essentially the Fermi momentum. Therefore we neglect the very weak three-momentum dependence of the gap and write it as  $\Delta(k_0)$ . We also write  $\mathbf{p} = \mathbf{p}_F + \mathbf{l}$ , where  $\mathbf{p}_F$  is on the Fermi surface and  $\mathbf{l}$  is perpendicular to it. For very large chemical potential and vanishingly small temperature it is adequate to use  $l \ll \mu$  and write the integration measure as  $\mu^2 dl d(\cos \theta) d\phi$ ; furthermore,  $|\mathbf{q}| = |\mathbf{k} - \mathbf{p}| \approx \sqrt{2}\mu(1 - \cos \theta)$ . The Matsubara sum can be replaced by an integral over Euclidean momentum  $p_4$  (see (3.71)). The integral over  $\phi$  is trivial, and the integral over  $l$  can be done by contour integration, picking up the pole of the diquark propagator:

$$\begin{aligned} \Delta(k_4) = & \frac{g^2 \mu^2}{12\pi^2} \int_{-\infty}^{\infty} dp_4 \int_{-1}^1 d\cos \theta \frac{\Delta(p_4)}{\sqrt{p_4^2 + \Delta^2(p_4)}} \\ & \times \left[ \frac{3 - \cos \theta}{q_4^2 + 2\mu^2(1 - \cos \theta) + G(q)} \right. \\ & \left. + \frac{1 + \cos \theta}{q_4^2 + 2\mu^2(1 - \cos \theta) + F(q)} \right] \end{aligned} \quad (8.118)$$

Here  $F$  and  $G$  are evaluated with  $q_4 = k_4 - p_4$  and  $|\mathbf{q}| = \sqrt{2}\mu(1 - \cos \theta)$ . In principle this gap equation should now be solved with no further approximations.

To get an idea of how the solution depends on the parameters we use the approximate forms for  $F$  and  $G$ ,

$$F(q) = m_{\text{el}}^2 \quad G(q) = i \frac{\pi q_4}{4|\mathbf{q}|} m_{\text{el}}^2 \quad (8.119)$$

in the limit  $0 \leq q_4 \ll |\mathbf{q}|$ . This means that the electric part of the interaction is screened on the momentum scale  $q_{\text{el}} = m_{\text{el}}$  while the magnetic part is screened on the scale  $q_{\text{mag}} = (\pi m_{\text{el}}^2 \Delta/4)^{3/2}$ . Integration over the

angle  $\theta$  gives the simplified gap equation

$$\Delta(k_4) = \frac{g^2}{18\pi^2} \int dp_4 \frac{\Delta(p_4)}{\sqrt{p_4^2 + \Delta^2(p_4)}} \times \left[ \ln \left( 1 + \frac{32\mu^3}{\pi m_{\text{el}}^2 |k_4 - p_4|} \right) + \frac{3}{2} \ln \left( 1 + \frac{4\mu^2}{m_{\text{el}}^2} \right) \right] \quad (8.120)$$

This integral equation can be converted to a differential equation and solved in the small- $g$  approximation. The asymptotic solution is

$$\Delta(k_4) \approx \Delta_0 \sin \left[ \frac{g}{3\sqrt{2}\pi} \ln \left( \frac{c\mu}{k_4} \right) \right] \quad k_4 > \Delta_0 \quad (8.121)$$

where

$$\begin{aligned} \Delta_0 &= 2c\mu \exp \left( -\frac{3\pi^2}{\sqrt{2}g} \right) \\ 2c &= \frac{512}{\pi} \left( \frac{\mu}{m_{\text{el}}} \right)^5 \\ &= 512\pi^4 g^{-5} \quad (N_f = 2) \end{aligned}$$

The amazing feature about this result is that the gap depends exponentially on  $1/g$ , not on  $1/g^2$  as it does in ordinary superconductivity. This feature emerges from the longer-range nature of the color magnetic field compared with the color electric field. This result was first obtained by Son [36]. It has important implications for the numerical value of the gap, and the critical temperature, since  $g$  should be small compared to unity for the whole analysis to make sense.

Equation (8.120) is an approximation of (8.118). Numerical solution of the latter equation for small  $g$  yields a gap that is well described by (8.121) but with an overall coefficient that is smaller by a factor 0.28. However, there are several approximations that would need to be relaxed in order to obtain an accurate value of the coefficient of  $g^{-5} \exp(-3\pi^2/\sqrt{2}g)$  for the gap. These include the diagonal contribution to the diquark self-energy (which modifies the quasiparticle dispersion relation), a renormalization-group improvement to obtain the proper choice of scale at which to evaluate the running coupling  $g \rightarrow \bar{g}(\mu)$ , and the use of dressed vertices in the Schwinger–Dyson equation. The first two of these have been done individually, and the third not at all. If these effects are ignored,  $\Delta_0$  at first decreases with increasing  $\mu$ , reaches a minimum of about 10 MeV at  $\mu = 1$  TeV, and then increases logarithmically with  $\mu$ . A plot of  $\Delta_0$  versus  $\mu$  (Figure 8.3) gives the scale of the gap, although its absolute magnitude is uncertain by a factor 2–4, increasingly so as  $\mu$  decreases.

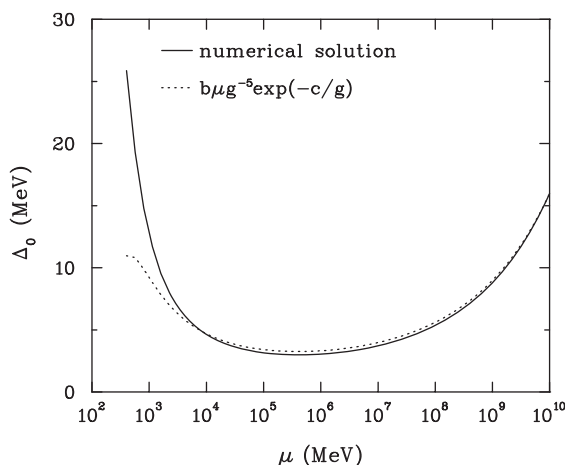


Fig. 8.3. The gap for two-flavor color superconductivity.

When color superconductivity occurs, the thermodynamic potential is lowered when compared with the case where pairing is absent. One may readily write an approximate expression for the thermodynamic potential that reproduces the Schwinger–Dyson equation used to obtain the gap equations. It is [37]

$$\begin{aligned} \Omega = \Omega_0 + \frac{1}{2}T \sum_n \int \frac{d^3p}{(2\pi)^3} \text{Tr} \left[ \ln \left( \frac{\mathcal{G}}{\mathcal{G}_0} \right) - \mathcal{G}\mathcal{G}_0^{-1} + 1 \right] \\ + \frac{1}{4}T^2 \sum_{n,n'} \int \frac{d^3p d^3p'}{(2\pi)^6} \Gamma_\mu^a(p, p') \mathcal{G}(p) \Gamma_\nu^b(p', p) \mathcal{G}(p') \mathcal{D}_{ab}^{\mu\nu}(p' - p) \end{aligned} \quad (8.122)$$

where  $\Omega_0$  is the potential in the absence of pairing. Treating  $\Omega$  as a functional of  $\mathcal{G}$  and requiring that it be an extremum results in  $\mathcal{G}^{-1} - \mathcal{G}_0^{-1} = \Sigma$ . When evaluated at the extremum, the shift in the potential (relative to no pairing) is

$$\delta\Omega = \frac{1}{2}T \sum_n \int \frac{d^3p}{(2\pi)^3} \text{Tr} \left[ \ln \left( \frac{\mathcal{G}}{\mathcal{G}_0} \right) - \frac{1}{2}\mathcal{G}\mathcal{G}_0^{-1} + \frac{1}{2} \right] \quad (8.123)$$

Using the explicit form of the propagator and integrating over spatial momentum, the zero-temperature shift in the energy density is

$$\delta\Omega = 4 \frac{\mu^2}{\pi^2} \int dp_4 \left[ \sqrt{p_4^2 + \Delta^2(p_4)} - p_4 - \frac{\Delta^2(p_4)}{2\sqrt{p_4^2 + \Delta^2(p_4)}} \right] \quad (8.124)$$

This expression requires numerical solution, but a very good approximation is

$$\delta\Omega(2\text{SC}) = -4 \left( \frac{\mu^2 \Delta_0^2}{4\pi^2} \right) \quad (8.125)$$

This was first obtained by Miransky, Shovkovy, and Wijewardhana [38]. The overall factor 4 comes from the pairing of four quarks in the 2SC state.

Now we turn to the case of three flavors of massless quarks. Numerous studies have shown that the energetically most favorable state is one in which rotations of SU(3) color and SU(3) flavor are locked together. This is referred to as color–flavor locking (CFL) [39]. The simplest ansatz for the gap matrix is

$$\Delta_{ij}^{ab}(p) = (\lambda_I)^{ab} (\lambda_I)_{ij} C \gamma_5 [\Delta_+(p)P_+(p) + \Delta_-(p)P_-(p)] \quad (8.126)$$

where  $\lambda_I$  is one of the three antisymmetric SU(3) matrices. The analysis then closely parallels the case of 2SC. It turns out that there are eight color–flavor combinations of quarks with gap  $\Delta/2^{1/3}$  and one with gap  $2\Delta/2^{1/3}$ , where  $\Delta$  is the same function as in 2SC. To logarithmic accuracy the CFL phase is favored over the 2SC phase at asymptotically high density, as long as  $m_s^2 \ll 2\mu\Delta_0$ :

$$\delta\Omega(\text{CFL}) = -\frac{12}{2^{2/3}} \left( \frac{\mu^2 \Delta_0^2}{4\pi^2} \right) \quad (8.127)$$

For these weak coupling estimates to be valid, one may require for example that  $g < 0.8$ . This translates to  $\mu > 100$  GeV, a density not relevant for any known terrestrial, astrophysical, or cosmological environment. What is of most interest for neutron stars and high-energy heavy ion collisions is the region of  $\mu$  in the range from several hundred MeV to several GeV (remember that  $\mu$  is one-third of the baryon chemical potential) and temperatures up to several hundred MeV. In this region of phase space, weak-coupling calculations may be a guide but cannot provide quantitative predictions. Therefore model studies have been done using the Nambu–Jona–Lasinio (NJL) model and instanton models for quark interactions. Figure 8.4 shows four likely phase diagrams depending on the number of quark flavors and the values of their masses. Panel (a) shows  $N_f = 2$  flavors of massless quarks. At low density and temperature there is a nuclear liquid–gas phase transition, to be discussed in Chapter 11: a curve showing a line of first-order phase transition terminates in a second-order transition at the dot. A second curve separates hadronic and nuclear matter from quark–gluon plasma (QGP) and cold quark matter; the phase transition is second order above a critical point indicated by

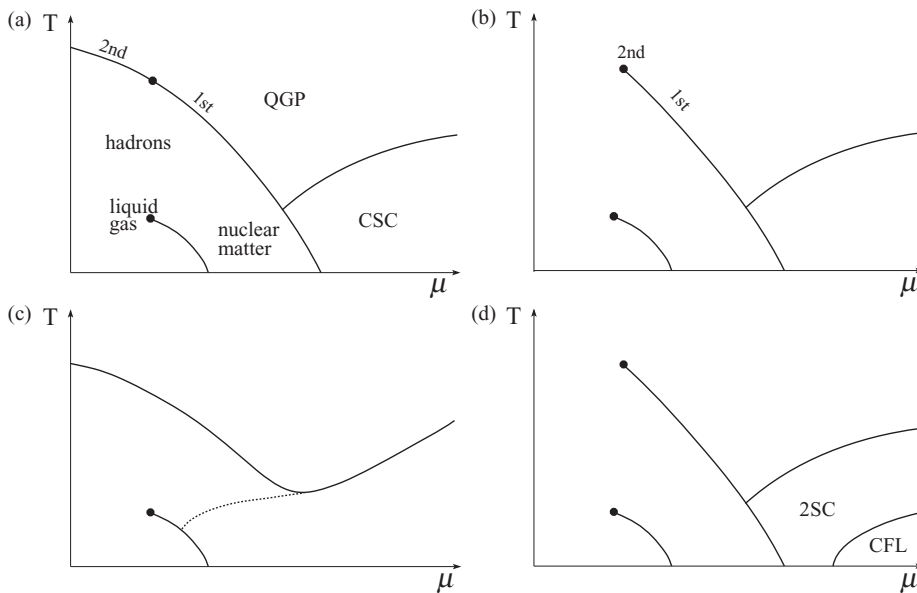


Fig. 8.4. A model study of the phase diagram ( $T$  as a function of  $\mu$ ) for strongly interacting matter. The two upper panels are for two flavors of quarks; in (a) both quarks are massless whereas in (b) their masses have a nonzero common value. The two lower panels are for three flavors of quarks. In (c) they all are massless, in (d) the up and down quark masses are equal and the strange quark is given a heavier mass. (From Schäfer [40].)

the dot and first order below it. Color superconductivity (CSC) exists at high density and small temperatures and is separated from an unpaired quark–gluon plasma by a third curve, a line of second-order phase transition.

Panel (b) is like panel (a) except that the up and down quark masses are given a nonzero common value. In this case the line of first-order phase transition terminates at the critical point; there are paths along which one can go from nuclear or hadronic matter to quark–gluon plasma without undergoing a phase transition.

Panel (c) shows a scenario for three massless quark flavors. There is a line of first-order phase transition starting at  $\mu = 0$  and extending to infinite density. At a given density, there is a high-temperature phase of quark–gluon plasma and a low-temperature phase which is either nuclear or hadronic or a CFL superconductor. Whether there is a sharp transition between dense nuclear matter and the CFL phase is unclear, as indicated by the dotted line.

Panel (d) shows a scenario for equal nonzero up and down quark masses and a heavier strange quark mass. The main difference between this panel and panel (b) is that, for a given temperature, the 2SC phase is favored at first and then the CFL phase is favored as the density increases. The non-superconducting phases and their phase transitions will be addressed more extensively in later chapters. The structure of strongly interacting matter is very rich and interesting!

### 8.10 Exercises

- 8.1 Prove that the QCD field strength tensor is not invariant under an infinitesimal gauge transformation, but that its square is.
- 8.2 Verify (8.26) by either of the two methods suggested.
- 8.3 Solve the renormalization-group equation for the covariant gauge parameter  $\bar{\rho}$ . Use (8.17), (8.18) with the one-loop results (8.22), (8.28).
- 8.4 Make graphs of (8.31) and (8.33), and then plot equations (8.34) to see how good an approximation they are.
- 8.5 Evaluate at least one of the non-quark two-loop diagrams for the pressure and show that it contributes to (8.45) as stated.
- 8.6 In the calculation of the pressure at order  $g^4$  with fermions, enumerate all the diagrams that contribute and determine their individual combinatoric factors.
- 8.7 When evaluating the static ( $k_0 = 0$ ) limit of the gluon polarization tensor  $\Pi_{\mu\nu}$ , one encounters integrals of the type

$$\int_0^\infty dx \left( \frac{1}{e^{ax} - 1} \right) \ln \left( \frac{1+x}{|1-x|} \right) \quad (\text{E8.1})$$

Derive the asymptotic  $a \rightarrow 0$  expansion for this integral, which is  $\frac{\pi^2}{2a} + \ln \left( \frac{a}{2\pi} \right) + \gamma_E + \mathcal{O}(a)$  *Hint:* Divide the range of integration into  $(0, 1)$  and  $(1, \infty)$ . Expand the logarithm in the integrand for each range appropriately and integrate term by term. Take the leading terms for  $a \rightarrow 0$  and sum the resulting series.

- 8.8 (8.100) was determined on the basis of loop diagrams containing only three-point vertices. Can you find diagrams containing only four-point vertices which give the same behavior?
- 8.9 Plot the pressure of pure gluons to order  $g^3$ , with  $g^2$  running with  $T$  according to the one-loop  $\beta$ -function. How much do the results change when the two-loop  $\beta$ -function is used instead?
- 8.10 Compare numerically the contribution to the pressure from instantons to the perturbative contribution at order  $g^2$ .
- 8.11 Calculate the dispersion relations for quarks in the 2SC phase.



## References

1. Politzer, H. D., *Phys. Rev. Lett.* **30**, 1346 (1973).
2. Gross, D. J., and Wilczek, F., *Phys. Rev. Lett.* **30**, 1343 (1973).
3. Yang, C. N., and Mills, R., *Phys. Rev.* **96**, 191 (1954).
4. Close, F. (1979). *Introduction to Quarks and Partons* (Academic Press, New York).
5. Georgi, H., and Politzer, H. D., *Phys. Rev. D* **14**, 1829 (1976).
6. Hagiwara, K., and Yoshino, T., *Z. Phys.* **C24**, 185 (1984).
7. Caswell, W. E., *Phys. Rev. Lett.* **33**, 244 (1974).
8. Collins, J. C., and Perry, J. M., *Phys. Rev. Lett.* **34**, 1353 (1975).
9. Shuryak, E. V., *Sov. Phys. JETP* **47**, 212 (1978).
10. Kapusta, J. I., *Nucl. Phys.* **B148**, 461 (1979).
11. Toimela, T., *Phys. Lett.* **B124**, 407 (1983).
12. Freedman, B. A., and McLerran, L. D., *Phys. Rev. D* **16**, 1130, 1147, 1169 (1977).
13. Baluni, V., *Phys. Rev. D* **17**, 2092 (1978).
14. Celmaster, W., and Sivers, D., *Phys. Rev. D* **23**, 227 (1981).
15. Arnold, P., and Zhai, C., *Phys. Rev. D* **51**, 1906 (1995); **50**, 7603 (1994).
16. Zhai, C., and Kastening, B., *Phys. Rev. D* **52**, 7322 (1995).
17. Kajantie, K., Laine, M., Rummukainen, K., and Schröder, Y., *Phys. Rev. D* **67**, 105008 (2003).
18. Leibbrandt, G., *Rev. Mod. Phys.* **59**, 1067 (1987).
19. Kajantie, K., and Kapusta, J. I., *Ann. Phys. (NY)* **160**, 477 (1985).
20. Heinz, U., Kajantie, K., and Toimela, T., *Ann. Phys. (NY)* **176**, 218 (1987).
21. Belavin, A. A., Polyakov, A. M., Schwartz, A. S., and Tyupkin, Yu. S., *Phys. Lett.* **B59**, 85 (1975).
22. 't Hooft, G., *Phys. Rev. D* **14**, 3432 (1976); Err. **18**, 2199 (1978).
23. Harrington, B. J., and Sheppard, H. K., *Phys. Rev. D* **17**, 2122 (1978).
24. Pisarski, R. D., and Yaffe, L. G., *Phys. Lett.* **B97**, 110 (1980).
25. Schäfer, T., and Shuryak, E. V., *Rev. Mod. Phys.* **70**, 323 (1998).
26. Lindé, A. D., *Phys. Lett.* **B96**, 289 (1980).
27. Braaten, E., *Phys. Rev. Lett.* **74**, 2164 (1995).
28. Farhi, E., and Jaffe, R. L., *Phys. Rev. D* **30**, 2379 (1984).
29. Madsen, J., *Lect. Notes Phys.* **516**, 162 (1999).
30. Barrois, B. C., *Nucl. Phys.* **B129**, 390 (1977).
31. Frautschi, S. (1980). *Proceedings of the Workshop on Hadronic Matter at Extreme Energy Density, Erice 1978* (Plenum Press, New York).
32. Bailin, D., and Love, A., *Nucl. Phys.* **B205**, 119 (1982).
33. Alford, M. G., Rajagopal, K., and Wilczek, F., *Phys. Lett.* **B422**, 247 (1998).
34. Rapp, R., Schäfer, T., Shuryak, E. V., and Velkovsky, M., *Phys. Rev. Lett.* **81**, 53 (1998).
35. Nambu, Y., *Phys. Rev.* **117**, 648 (1960); Gorkov, L. P., *Sov. Phys. JETP* **9**, 1364 (1959).
36. Son, D. T., *Phys. Rev. D* **59**, 094019 (1999).

37. Schäfer, T., *Nucl. Phys.* **B575**, 269 (2000).
38. Miransky, V. A., Shovkovy, I. A., and Wijewardhana, L. C. R., *Phys. Lett.* **B468**, 270 (1999).
39. Alford, M. G., Rajagopal, K., and Wilczek, F., *Nucl. Phys.* **B537**, 443 (1999).
40. Schäfer, T., *Int. J. Mod. Phys.* **B15**, 1474 (2001).

## Bibliography

### Reviews of QCD (at zero and finite temperature)

- Politzer, H. D., *Phys. Rep.* **141**, 129 (1974).
- Close, F. (1979). *Introduction to Quarks and Partons* (Academic Press, New York).
- Shuryak, E. V., *Phys. Rep.* **61**, 71 (1980).
- Gross, D. Pisarski, R., and Yaffe, L., *Rev. Mod. Phys.* **53**, 43 (1981).
- Smilga, A. V. (2001). Hot and Dense QCD, in *At the Frontiers of Particle Physics: Handbook of QCD* (World Scientific, Singapore).